ORIGINAL ARTICLE

Gene expression networks in COPD: microRNA and mRNA regulation

Michael E Ezzie,[1] Melissa Crawford,[1] Ji-Hoon Cho,[2] Robert Orellana,[1] Shile Zhang,[2] Richard Gelinas,[2] Kara Batte,[1] Lianbo Yu,[1] Gerard Nuovo,[1] David Galas,[2] Philip Diaz,[1] Kai Wang,[2] S Patrick Nana-Sinkam[1]

► Additional data are published online only. To view these files please visit the journal online (http://thorax.bmj.com/content/67/2.toc).

[1]Department of Medicine, Dorothy M. Davis Heart and Lung Research Institute, The Ohio State University Medical Center, Columbus, Ohio, USA
[2]Institute for Systems Biology, Seattle, Washington, USA

Correspondence to
Dr S Patrick Nana-Sinkam, Ohio State University Medical Center, Davis HLRI, 473 W 12th Ave, Room 201, Columbus, OH 43210, USA; patrick.nana-sinkam@osumc.edu

ME and MC contributed equally to this manuscript.

Received 24 February 2011
Accepted 21 August 2011
Published Online First 22 September 2011

ABSTRACT

Background The mechanisms underlying chronic obstructive pulmonary disease (COPD) remain unclear. MicroRNAs (miRNAs or *miRs*) are small non-coding RNA molecules that modulate the levels of specific genes and proteins. Identifying expression patterns of miRNAs in COPD may enhance our understanding of the mechanisms of disease. A study was undertaken to determine if miRNAs are differentially expressed in the lungs of smokers with and without COPD. miRNA and mRNA expression were compared to enrich for biological networks relevant to the pathogenesis of COPD.

Methods Lung tissue from smokers with no evidence of obstructive lung disease (n=9) and smokers with COPD (n=26) was examined for miRNA and mRNA expression followed by validation. We then examined both miRNA and mRNA expression to enrich for relevant biological pathways.

Results 70 miRNAs and 2667 mRNAs were differentially expressed between lung tissue from subjects with COPD and smokers without COPD. miRNA and mRNA expression profiles enriched for biological pathways that may be relevant to the pathogenesis of COPD including the transforming growth factor β, Wnt and focal adhesion pathways. miR-223 and *miR-1274a* were the most affected miRNAs in subjects with COPD compared with smokers without obstruction. *miR-15b* was increased in COPD samples compared with smokers without obstruction and localised to both areas of emphysema and fibrosis. *miR-15b* was differentially expressed within GOLD classes of COPD. Expression of SMAD7, which was validated as a target for *miR-15b*, was decreased in bronchial epithelial cells in COPD.

Conclusions miRNA and mRNA are differentially expressed in individuals with COPD compared with smokers without obstruction. Investigating these relationships may further our understanding of the mechanisms of disease.

Key messages

What is the key question?

- Chronic obstructive pulmonary disease (COPD) is a worldwide health crisis mostly attributable to cigarette smoking.
- The precise mechanisms underlying COPD development are not clear, but genomic and proteomic studies are improving our understanding of the pathogenesis of this disease.
- Researchers have identified abnormal expression of microRNAs (miRNAs or miRs) in several types of cancers, but our knowledge of the significance of these small molecules in diseases other than cancer including COPD is just emerging.

What is the bottom line and why read on?

- 70 miRNAs that were differentially expressed in lung tissue from smokers without COPD and those with COPD (GOLD stages 1, 2 and 4) were identified.
- The correlation between differentially expressed miRNAs and genes suggests potentially functionally relationships that may contribute to the pathogenesis of COPD.

INTRODUCTION

Chronic obstructive pulmonary disease (COPD) is a worldwide epidemic primarily attributable to the effects of cigarette smoke. It is a heterogeneous disease defined by airflow limitation that is not fully reversible and an abnormal inflammatory response of the lung to noxious stimuli.[1] Mechanisms implicated include those directly attributable to the effects of cigarette smoke such as cellular injury, inflammation and abnormal repair.[2]

MicroRNAs (miRNAs, *miR*) are one member of a family of small non-coding RNAs (approximately 21–25 nucleotides long) encoded in the genome of organisms ranging from animals and plants to viruses.[3] These molecules represent components of the human genome that were previously thought to be non-functional. miRNAs are integral to key biological functions and modulate both gene and protein levels by either destabilising transcripts or inhibiting protein translation. Given the relative redundancy of complementary sequences between miRNAs and their target mRNA, single miRNAs have the capacity to regulate tens to hundreds of genes simultaneously. In fact, it is estimated that miRNAs may target up to one-third of the transcriptome.[4]

miRNA deregulation has been implicated in the pathogenesis of several diseases including both haematological and solid malignancies. miRNA expression patterns in primary tumour tissues, blood, sputum and urine are being investigated as biomarkers for both diagnosis and prognosis in disease. These miRNA signatures may eventually be applied to clinical practice. Our knowledge of the role of miRNAs in the pathogenesis of lung

Table 1 Demographic characteristics of study patients

	Normal smokers (N=9)	GOLD 1 (N=7)	GOLD 2 (N=9)	GOLD 4 (N=10)	p Value
Men (%)	44	42.8	44	60	0.880
Age	63.22±11.43	69.71±7.39	69.11±7.30	50.90±5.62	<0.0001
Pack-years of smoking	25.67±16.70	41.86±23.26	44.00±20.15	56.40±36.42	0.106
SGRQ score	11.86±17.27	31.90±19.35	36.79±16.79	61.05±15.62	<0.0001
BMI	28.76±6.81	26.97±4.10	26.50±5.23	24.88±2.59	0.409
FEV_1 PD	104.22±15.50	89.00±5.77	70.56±5.05	21.20±7.96	<0.0001

BMI, body mass index; FEV_1 PD, forced expiratory volume in 1 s percentage predicted; NA, not available; SGRQ, St George Respiratory Questionnaire score.

disease is rapidly expanding, and miRNAs appear to be important in maintaining homeostasis during lung development and may have a pathogenic role in lung disease.[5 6] In addition, miRNAs may be involved in the regulation of inflammation in the lung in response to exogenous stimuli in animal models.[7 8]

Little is known regarding the role of miRNAs in COPD. Two studies have investigated the effects of cigarette smoke on miRNA expression.[9 10] In the first study 24 miRNAs were significantly downregulated between smoke-exposed rats and sham groups.[9] In the second study the effects of smoke exposure on miRNA expression in mice were investigated.[10] The majority of deregulated miRNAs in this study were also downregulated.

Similar studies are being conducted in specific cell types in smokers and subjects with COPD. Schembri *et al* compared miRNA and mRNA expression in airway epithelial cells from smokers versus never smokers.[11] Twenty-eight miRNAs were differentially expressed, with the majority downregulated in smokers. Sato *et al* examined the expression of *miR-146a* in fibroblasts from subjects with and without COPD.[12] *miR-146a* expression in cultured fibroblasts was reported to correlate with COPD severity as assessed by expiratory airflow.

Our goal in this study was to determine if miRNAs were differentially expressed in the lungs of patients with COPD and if miRNA expression may be linked to mRNA expression and thus biological pathways relevant to the pathogenesis of COPD. We compared miRNA and mRNA expression patterns in lung tissue from subjects with different Global Initiative for Obstructive Lung Disease (GOLD) stages of COPD and smokers without airflow limitation. We enriched for predicted miRNA targets in our group of deregulated mRNAs. Lastly, we identified transforming growth factor (TGF)-β, Wnt and focal adhesion pathways as potential pathways in which miRNAs may be relevant to the pathogenesis of COPD.

METHODS

Additional details of methods are shown in the online supplement.

Subject selection

Thirty-five tissue samples were procured through a Lung Tissue Research Consortium approved project (#07-99-0008) for the purposes of miRNA and mRNA analysis. Clinical information available for the subjects included age, gender, height, weight and smoking history. Test results including spirometry, pathological diagnosis and the results of the St George Respiratory Questionnaire health surveys were available.

Tissue processing and RNA isolation

Total RNA was isolated from frozen tissue samples using a freeze fracture protocol, followed by Trizol extraction and precipitation at −20°C overnight to increase the yield of small RNAs. RNA integrity was determined by capillary electrophoresis on an Agilent 2100 Bioanalyzer. Only RNA with an integrity number ≥7 was used in the profiling studies.

miRNA microarray

miRNAs were profiled in subjects with COPD (N=19) and normal smokers (N=8) using Exiqon miRNA microarrays according to the manufacturer's instructions (Exiqon, Woburn, Massachusetts, USA). The labelled miRNA probes were hybridised to the miRCURY LNA arrays v.11.0 for 16 h at 56°C. After hybridisation the arrays were washed and scanned at 5 μm resolution using a ScanArray Express (Perkin Elmer, Waltham, Massachusetts, USA).

Messenger RNA microarray

Samples were prepared for mRNA microarray analysis using Agilent Quick Amp Labeling technologies (Santa Clara, California, USA). Hybridised slides were then washed and scanned with ScanArray Express (Perkin Elmer).

mRNA and miRNA microarray data processing

For mRNA data, raw intensities from all samples were merged, normalised using the quantile method and transformed into $\log_2$ scale.[13] Present probes with mean intensity over all samples larger than the global mean intensity were chosen and used for

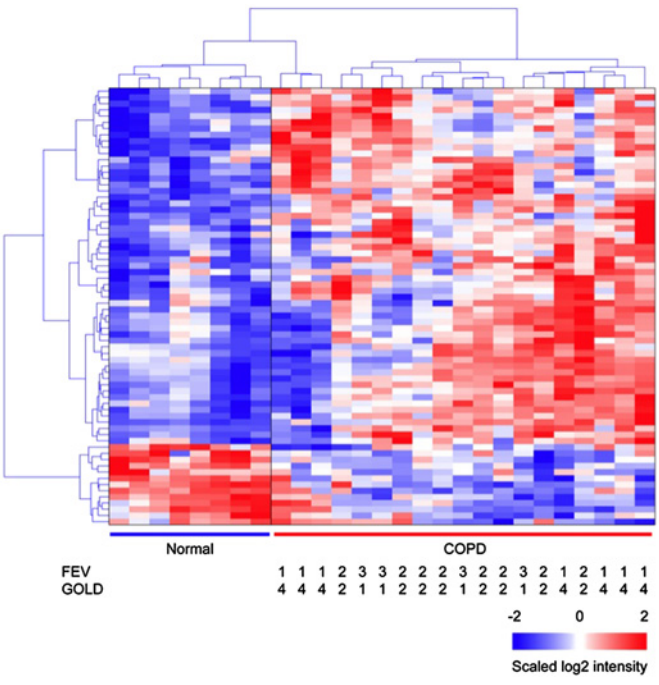

Figure 1 Hierarchical clustering result of differentially expressed microRNAs (miRNAs) in lungs from subjects with chronic obstructive pulmonary disease (COPD) compared to smokers without COPD. Exiqon miRCURY LNA microRNA Array v11 was used for miRNA expression profiling. Seventy differentially expressed miRNAs (DEmiRNAs) were identified between COPD samples (n=19) and smokers without obstruction (n=8) which showed a positive false discovery rate <0.05 and fold changes >±1.5 using the LIMMA method.

Table 2 Top 10 upregulated microRNAs in lungs from subjects with COPD compared with smokers without COPD

	Fold difference (COPD/normal smokers)	p Value	pFDR value
hsa-miR-223	2.93	6.63E-04	1.37E-03
hsa-miR-1274a	2.73	3.19E-10	4.44E-09
hsa-miR-144	2.38	2.83E-03	4.26E-03
hsa-miR-374a	2.25	1.72E-04	4.74E-04
hsa-miR-664	2.21	2.00E-08	2.02E-07
hsa-miR-148a	2.15	2.34E-07	1.68E-06
hsa-miR-766	2.06	1.05E-05	4.76E-05
hsa-miR-486-5p	2.05	3.26E-04	8.21E-04
hsa-miR-10a	2.05	7.47E-04	1.46E-03
hsa-miR-451	2.00	5.39E-02	4.59E-02

COPD, chronic obstructive pulmonary disease; pFDR, positive false discovery rate.

Table 3 Top 10 downregulated microRNAs in lungs from subjects with COPD compared with smokers without COPD

miRNA	Fold difference (COPD/normal smokers)	p Value	pFDR value
hsa-miR-923	−5.06	5.88E-06	2.91E-05
hsa-miR-937	−2.36	1.89E-06	1.08E-05
hsa-miR-422a	−2.12	1.45E-06	8.74E-06
hsa-miR-576-3p	−2.06	1.57E-06	9.22E-06
hsa-miR-513a-5p	−2.06	3.57E-04	8.54E-04
hsa-miR-25*	−2.01	2.10E-07	1.56E-06
hsa-miR-99b*	−1.81	1.23E-05	5.25E-05
hsa-miR-125b-1*	−1.75	1.38E-05	5.70E-05
hsa-miR-24	−1.75	1.59E-04	4.49E-04
hsa-miR-187*	−1.64	3.14E-04	8.04E-04

*indicates miRNA on the opposite arm of the hairpin during processing.
COPD, chronic obstructive pulmonary disease; pFDR, positive false discovery rate.

further statistical analysis. LIMMA[14] and QVALUE[15] R packages were used to perform statistical testing of differential mRNA and miRNA expression between control smoker and COPD samples and to compute the positive false discovery rate (pFDR), respectively. Present probes were used for statistical testing to increase the ratio of true positives to false positives,[16] and differentially expressed mRNAs and miRNAs were defined as having a pFDR <0.05 with at least ±1.5-fold change between the groups.

Quantitative reverse transcription PCR validation

Independent assays were performed using quantitative reverse transcription PCR (qRT-PCR) on all patient samples for individual miRNA (*miR-15b*, *miR-223*, *miR-1274a* and *miR-424*) and mRNA (telomerase associated protein 1 (TEP1), interleukin 6 (IL-6), catalase (CAT) and mothers against decapentaplegic homologue 7 (Drosophila) (SMAD7) (Applied Biosystems, Foster City, California, USA). All RT-PCR experiments were performed in three independent experiments conducted in triplicate on all study samples. Data were presented relative to either 18s for mRNA or U43 for miRNA based on calculations of $2^{(-\Delta Ct)}$. Statistical significance was defined as $p<0.05$ as measured by the Student t test or ANOVA (see tables E1 and E2 in online supplement for sequences of miRNA and mRNA probes).

Functional enrichment study

In order to identify Kyoto Encyclopedia of Genes and Genomes (KEGG)[17] pathways associated with a set of genes, we used DAVID[18] and obtained the list of enriched pathways. Their p values were computed by a modified Fisher exact test called the EASE score method.[18]

Target prediction and network analysis

Predicted target genes for miRNAs were obtained using TargetScan v5.1, PicTar and miRanda. For differentially expressed miRNAs, all predicted targets in human genes and predicted targets overlapping with differentially expressed genes were used to perform KEGG pathway enrichment analysis. To describe the potential relationship between differentially expressed genes and miRNAs in a KEGG pathway, the predicted miRNA gene pairs from TargetScan showing negative expression correlations (<−0.5) were incorporated into the pathway diagram. A modified KEGG pathway diagram was generated using Cytoscape.[19]

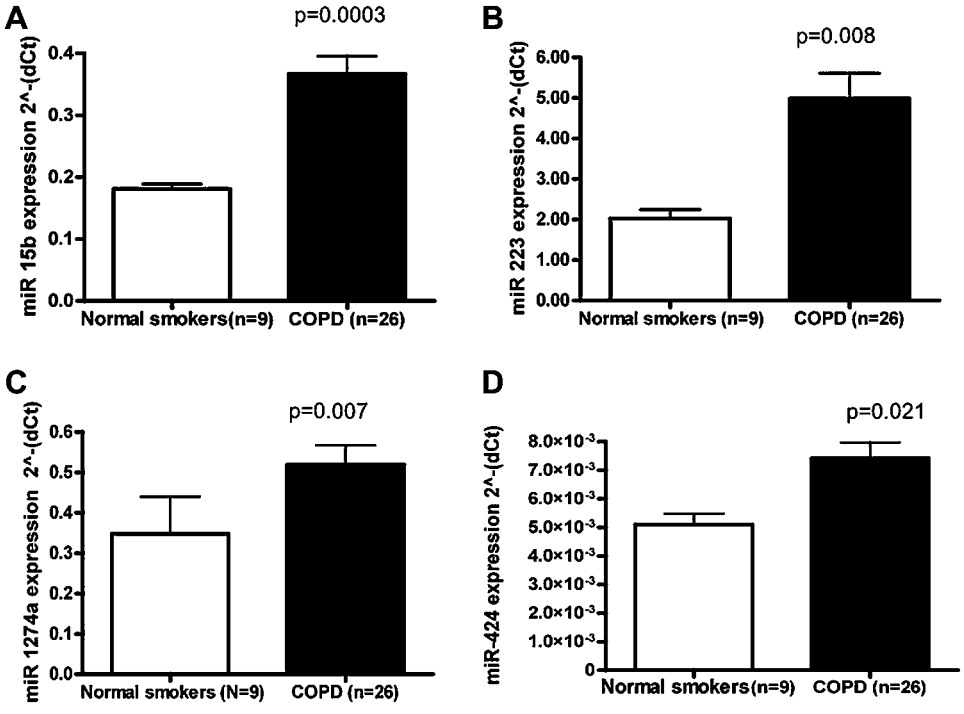

Figure 2 Quantitative reverse transcription polymerase chain reaction (qRT-PCR) validation of differentially expressed microRNAs (miRNAs). qRT-PCR was performed on the same RNA samples (nine normal smokers and 26 subjects with chronic obstructive pulmonary disease) by individual miRNA for (A) *miR-15b*, (B) *miR-223*, (C) *miR-1274a* and (D) *miR-424*. All RT-PCR experiments were performed in two independent experiments conducted in triplicate. Data are presented as $2^{(-\Delta Ct)}$ relative to U43. There was a statistically significant difference as measured by the Student t test in subjects with chronic obstructive pulmonary disease (COPD) compared with normal smokers for *miR-15b*, *miR-223*, *miR-1274a* and *miR-424*.

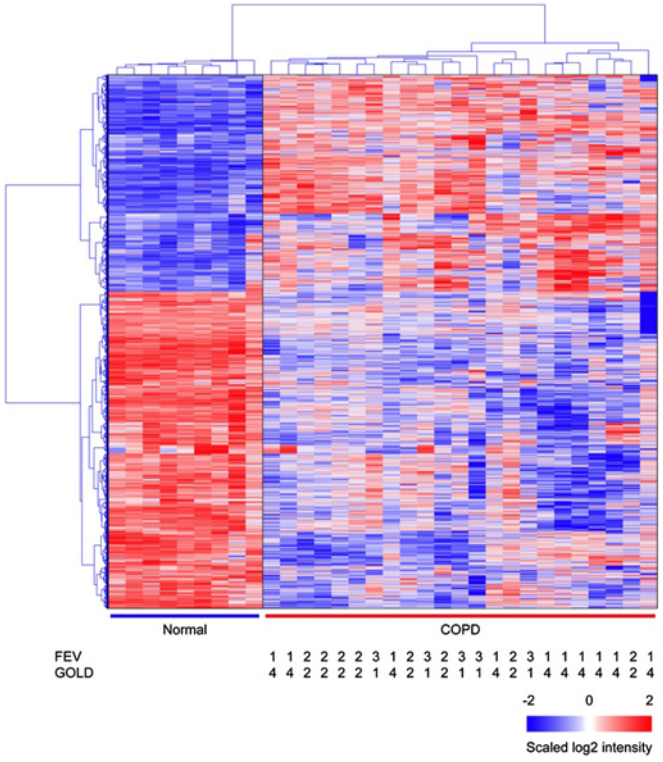

Figure 3 Hierarchical clustering result of differentially expressed genes in subjects with chronic obstructive pulmonary disease (COPD) compared with smokers without COPD. There were 2667 differentially expressed genes between subjects with COPD (N=23) and smokers without COPD (N=9). Hierarchical clustering result showed the clear separation of COPD patient samples from smokers without COPD samples. Normal: smokers without airflow limitation.

In situ hybridisation and co-localisation

Co-localisation analyses of SMAD7, cytokeratin AE 1/3 and *miR-15b* expression were conducted as previously described.[20] After development the slide was analysed with the Nuance system (Cambridge Research and Instrumentation, Hopkinton, MA). The Nuance system converts the blue and brown signals to fluorescent blue and red, respectively, then mixes them to determine if a given cell contains both targets. The negative controls were the omission of the probe and the use of a scrambled probe, as previously described.[20]

Transfection studies and western blot analyses

Details of transfection studies and western blot analyses are shown in the online supplement.

TGFβ treatment

Beas2B cells were transfected with either scrambled or pre-miR15b as described above. 72 h after transfection the cells were starved for 6 h followed by treatment with TGFβ (5 ng/ml; Sigma, St Louis, Missouri, USA). The cells were harvested at 10, 15 and 30 min and assessed for phosphorylated SMAD 3 protein expression (Cell Signaling, Danvers, Massachusetts, USA).

Migration assay

The migration rate was assayed using the IBIDI culture insert (München, Germany). Images were taken on an Olympus IX81 immediately (time 0) and again at 8 and 24 h. Seven random widths were measured across the wound at time 0. The number of pixels was converted to microns and the line was then superimposed onto the subsequent time points. The mean and SD of the seven lines was calculated using ImageJ software to determine the distance of wound closure. Experiments were performed in triplicate.

RESULTS

Study subjects

Tissue samples were obtained from subjects with GOLD stages 1, 2 and 4 COPD (N=26) and from smokers without evidence of obstruction (N=9) from the Lung Tissue Research Consortium. There were no pathological or clinical diagnoses of cancer across the COPD or control tissue specimens. GOLD stage 4 tissue was obtained from explanted lungs. Tissue from smokers without airflow obstruction and GOLD stages 1 and 2 tissue was obtained mainly by wedge resection with pathology showing no evidence of cancer. Demographic information is presented in table 1 with accompanying summary statistics for each group.

There was an overall difference between the mean ages of all subjects ($p<0.0001$). Subjects with GOLD stage 4 COPD were younger than those with GOLD 1 COPD ($p<0.001$), GOLD 2 COPD ($p<0.001$) and smokers without airflow limitation

Table 4 Top 10 upregulated mRNA in lung tissue from subjects with COPD compared with smokers without COPD

Gene ID	Gene title	Gene symbol	Fold difference (COPD/normal smokers)	p Value	pFDR value	Function
9507	ADAM metallopeptidase with thrombospondin type 1 motif, 4	ADAMTS4	8.91	2.16E-04	4.02E-04	Proteolytic activity
7011	Telomerase-associated protein 1	TEP1	7.24	4.88E-13	5.06E-11	Alternative splicing, nucleo-cytoplasmic transport
10949	Heterogeneous nuclear ribonucleoprotein A0	HNRNPA0	6.86	8.02E-22	5.24E-18	mRNA processing, transport and metabolism
2304	Forkhead box E1 (thyroid transcription factor 2)	FOXE1	6.30	4.02E-05	1.01E-04	Transcription factor, thyroid gland organogenesis
4001	Lamin B1	LMNB1	6.05	8.44E-12	4.52E-10	Nuclear stability, chromatin structure
117245	HRAS-like suppressor family, member 5	HRASLS5	5.26	1.59E-17	1.44E-14	Transferase, catalytic activity
3569	Interleukin 6 (interferon, beta 2)	IL6	5.18	1.50E-03	2.01E-03	Inflammation, B cell differentiation
6280	S100 calcium binding protein A9	S100A9	5.14	8.17E-07	4.14E-06	Cell cycle progression, differentiation, immune system
6696	Secreted phosphoprotein 1 (osteopontin, bone sialoprotein I, early T lymphocyte activation 1)	SPP1	5.10	6.58E-05	1.51E-04	Metabolic process, cellular organisation, binding
27097	TAF5-like RNA polymerase II, p300/CBP-associated factor (PCAF)-associated factor, 65 kDa	TAF5L	4.95	2.05E-12	1.51E-10	Histone acetylase

COPD, chronic obstructive pulmonary disease; pFDR, positive false discovery rate.

Table 5 Top 10 downregulated mRNA in lung tissue from subjects with COPD compared with smokers without COPD

Gene ID	Gene title	Gene symbol	Fold difference (COPD/normal smokers)	p Value	pFDR value	Function
22870	SAPS domain family, member 1	SAPS1	−4.46	3.15E-03	3.69E-03	Protein phosphatase
6435	Surfactant, pulmonary-associated protein A1B	SFTPA1B	−4.23	2.90E-08	2.76E-07	Binds surfactant phospholipids
5507	Protein phosphatase 1, regulatory (inhibitor) subunit 3C	PPP1R3C	−4.17	3.99E-05	1.01E-04	Glycogen-targeting subunit, increases glycogen
2662	Growth differentiation factor 10	GDF10	−4.14	3.07E-05	8.04E-05	TGFβ signalling
5350	Phospholamban	PLN	−3.93	1.78E-06	7.72E-06	Calcium regulation
25928	Sclerostin domain containing 1	SOSTDC1	−3.87	2.68E-04	4.79E-04	Inhibits TGFβ signaling and enhances Wnt signalling
9353	Slit homologue 2 (Drosophila)	SLIT2	−3.48	4.32E-08	3.81E-07	Cell migration and axonal navigation
4094	v-maf musculoaponeurotic fibrosarcoma oncogene homologue (avian)	MAF	−3.46	1.41E-06	6.35E-06	Transcriptional activator or repressor, oncogene or tumor suppressor depending on context
123624	ATP/GTP binding protein-like 1	AGBL1	−3.37	7.95E-06	2.66E-05	Tubulin processing
4629	Myosin, heavy chain 11, smooth muscle	MYH11	−3.31	2.09E-06	8.78E-06	Contractile protein

COPD, chronic obstructive pulmonary disease; pFDR, positive false discovery rate; TGFβ, transforming growth factor β.

(p=0.013) (see table E6 in online supplement). There was no overall difference in pack years between the groups (p=0.106). Subjects with GOLD stage 4 tended to have more smoke exposure than smokers without airflow limitation (p=0.068; see table E7 in online supplement). The overall difference in scores on the St George Respiratory Questionnaire and forced expiratory volume in 1 s percentage predicted were significant (p<0.0001) as expected (see table E8 in online supplement).

MicroRNAs are differentially expressed between COPD and control lung tissues

Seventy miRNAs were differentially expressed between COPD tissue (N=19) and tissue from smokers without airflow limitation (N=8), as shown in figure 1. Thirteen miRNAs were downregulated in COPD tissue and 57 were upregulated. *miR-223* and *miR-1274a* were increased in expression by nearly threefold in COPD samples compared with smokers without airflow limitation (table 2). *miR-923* had an average decrease in expression of fivefold in COPD tissue compared with tissue from smokers without airflow limitation (table 3).

QT-PCR validation of differentially expressed microRNAs between COPD and control lung tissues

We validated miRNAs *(miR-15b*, *miR-223*, *miR-1274a* and *miR-424*) by qRT-PCR, as shown in figure 2. *miR-223* and *miR-1274a* were chosen for further validation based on dramatic increases in expression in COPD samples. *miR-15b* and *miR-424* were chosen for validation based on target prediction results and the potential role of these miRNAs in enriched pathways including TGF-β. The expression of *miR-223*, *miR-1274a*, *miR-15b* and *miR-424* was verified by quantitative PCR between all COPD samples (n=26) and all tissue samples from smokers without airflow limitation (n=9) and found to be of statistical significance (figure 2).

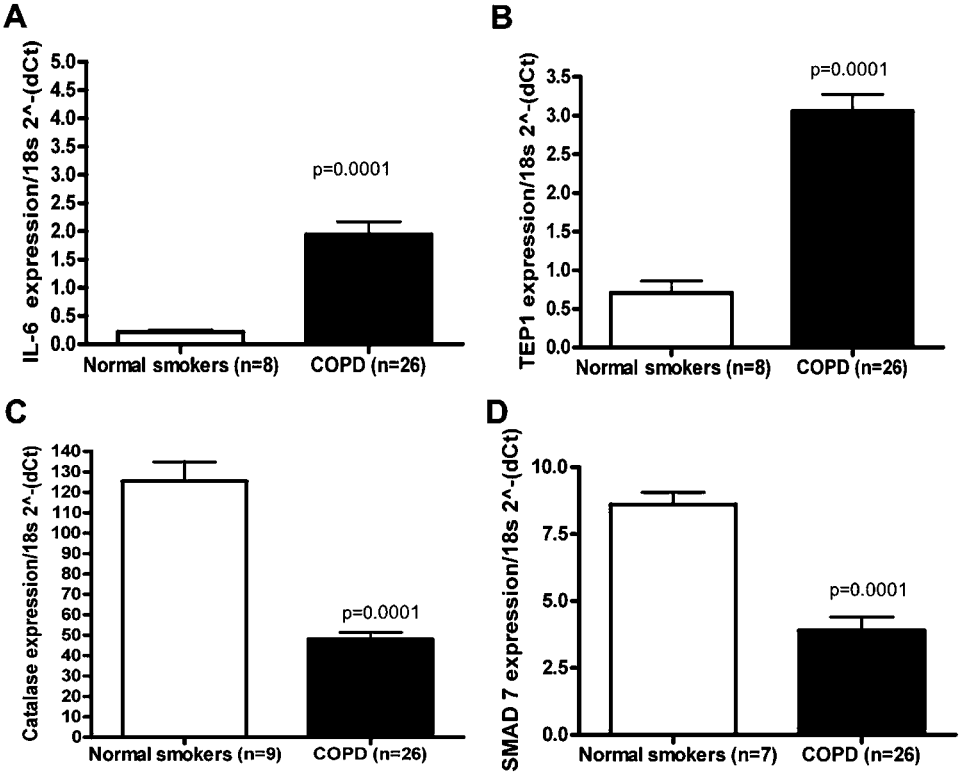

Figure 4 Quantitative reverse transcription polymerase chain reaction (qRT-PCR) validation of differentially expressed mRNAs. qRT-PCR was performed on the same RNA samples by mRNA TaqMan assay for (A) interleukin 6 (IL-6); (B) telomerase associated protein 1 (TEP1); (C) catalase (CAT) and (D) mothers against decapentaplegic homologue 7 (Drosophila) (SMAD7). All RT-PCR experiments were performed in three independent experiments conducted in triplicate. Data are presented as $2^{(-\Delta Ct)}$ relative to 18s RNA. In cases in which p<0.0001, values are presented as p=0.0001.

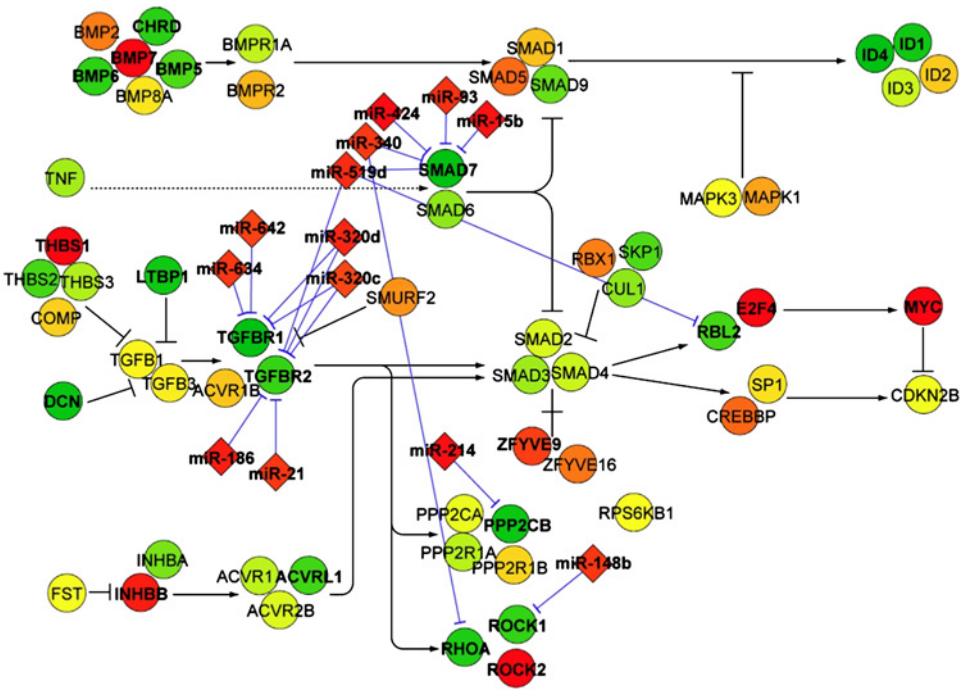

Figure 5 Transforming growth factor β (TGFβ) pathway in chronic obstructive pulmonary disease. Network representing TGFβ pathway was manually curated by combining KEGG pathway information and predicted targets of DEmiRNAs. Nodes represent deregulated genes (circles) in the pathway and DEmiRNAs (diamonds) predicted to be associated with the pathway. Node colours (red, upregulated; green, downregulated) represent fold changes of the corresponding genes. Deregulated genes and DEmiRNAs are indicated by bold symbols.

mRNAs are differentially expressed between COPD and control lung tissues

A comparison of microarray hybridisation results of 23 COPD lung samples and nine samples from smokers without airflow limitation revealed a total of 2667 genes that differed in expression between the two groups (fold change $>\pm1.5$ and pFDR <0.05; figure 3). Tables 4 and 5 show the 10 genes with the largest fold changes in each direction and their known biological function in expression between COPD tissue and tissue from smokers without airflow limitation.

qRT-PCR validation of differentially expressed genes between COPD and control lung tissues

The levels of IL-6, TEP1, CAT and SMAD7 were selected to be verified by qRT-PCR (figure 4). SMAD7, which has been investigated in the pathogenesis of COPD,[21] was markedly decreased in expression based on microarray analysis and validated by qRT-PCR (figure 4). As previously described in the literature, IL-6[22 23] was increased in COPD samples compared with smokers without airflow limitation, while CAT[24] was decreased. TEP1, a mammalian protein that is associated with telomerase activity, was significantly increased in expression in our COPD samples compared with controls (figure 4). Matrix metalloproteinase-9,[25] tumour necrosis factor α-induced protein 3 (TNFAIP3),[26] CSF3[27] and thrombospondin-1 (THBS1)[28] were also validated as increased in COPD samples compared with smokers without airflow limitation (data not shown).

TGFβ and WNT pathways are enriched by miRNA and mRNA expression profiling

We identified putative miRNA interacting targets using Targetscan, miRanda and PicTar which revealed interacting pairs between differentially expressed miRNAs (DEmiRNAs) and differentially expressed genes (DEGs). Among these pathways, Wnt, TGFβ signalling and focal adhesion pathways were significantly enriched by DEGs themselves and DEmiRNA-targeted DEGs predicted by three methods (see table E4 in online supplement).

Studies to date suggest a role for TGFβ in the pathogenesis of COPD,[29] and there are also current reports linking the Wnt pathway to COPD.[30] In figure 5, THBS1, inhibin β B (INHBB), Rho-associated coiled-coil containing protein kinase (ROCK) 2, SMAD-specific E3 ubiquitin protein ligase 1 (SMURF1), bone morphogenetic protein 7 (BMP7) and E2F transcription factor 4 (E2F4) were upregulated in COPD (red) while activin A receptor type I (ACVR1), SMAD7, ROCK1, latent TGFβ binding protein 1 (LTBP1), TGFβ receptor (TGFBR) 1 and TGFBR2 were downregulated (green). Several differentially expressed genes that are potential targets of differentially expressed miRNAs in the same tissue in the Wnt and focal adhesion pathways are shown in figures E2 and E3 in the online supplement. We chose to focus further attention on the interaction between *miR-15b* and SMAD7.

miR-15b localises to bronchial epithelium in COPD tissue

Based on in situ hybridisation for *miR-15b* in a representative case of a smoker with COPD as depicted in figure 6, *miR-15b* localised to both the bronchial epithelium and alveolar wall in type II pneumocytes (figure 6B,D). In addition, *miR-15b* was evident in areas of emphysema as well as fibrosis (figure 6E). Minimal SMAD7 was detectable in these same regions. However, we detected SMAD7 in normal bronchial epithelium and stromal cells (figure 6G,H). Importantly, co-localisation studies using Nuance co-labelling showed that the expression of SMAD7 was decreased in the presence of *miR-15b* (figure 7). Co-localisation *miR-15b* and the epithelial-specific AE 1/3 demonstrated an intense yellow signal, thus serving as a positive control (figure 7E,F).

miR-15b targets SMAD7 in bronchial epithelial cells and alters TGFβ signalling

SMAD7 is a predicted target of *miR-15b* (figure 8A). Overexpression of *miR-15b* in Beas2B bronchial epithelial cells resulted in decreased SMAD7, decorin and SMURF2 protein expression (figure 8B). Knockdown of *miR-15b* resulted in increased SMAD7, decorin and SMURF2 proteins. SMAD7 functions as an inhibitory SMAD in TGFβ signalling. We therefore sought to determine if *miR-15b* manipulation and thus SMAD7 expression would alter the cellular response to TGFβ. *miR-15b* overexpressing Beas2B cells exhibited increased early phosphorylated

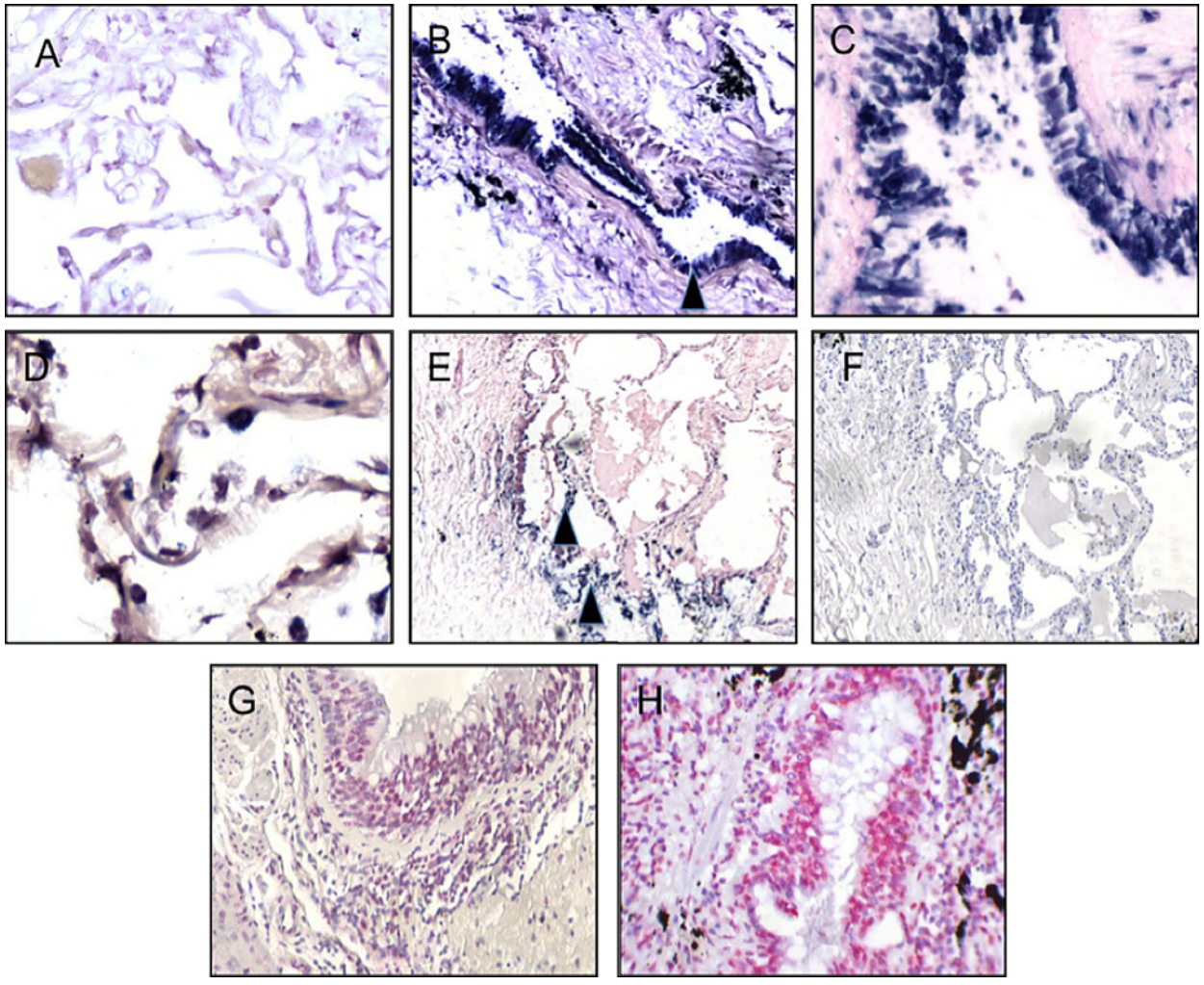

Figure 6 In situ hybridisation for mature *miR-15b*. Correlation of *miR-15b* and mothers against decapentaplegic homologue 7 (Drosophila) (SMAD7) expression with lung histopathology. (A) Lack of expression of scrambled miRNA as a control. (B) Normal lung where the *miR-15b* signal is intense in the epithelial cells of larger bronchi (arrowhead) (each image at 200×). (C) Same area at higher magnification (400×) where a nuclear and cytoplasmic signal is evident. (D) *miR-15b* signal in alveoli in a patient with emphysema and increased lung fibrosis (400×). (E) *miR-15b* in epithelial cells at the junction of areas of emphysema and fibrosis (arrowheads) (50×). (F) Same region showing no SMAD7 (50×). (G) SMAD7 in normal regions of bronchial epithelium (red stain) (100×). (H) Distribution of SMAD7 protein in a normal larger bronchus in a section of lung (200×). The nuclear-based signal involves primarily bronchial epithelial cells and mononuclear cells in the adjacent lymphoid infiltrate.

SMAD3 in response to TGFβ treatment. (figure 8C). *miR-15b* knockdown had the opposite effect with reduced early phosphorylation of SMAD3 (figure 8C) Lastly, we examined the effects of *miR-15b* on Beas2B proliferative and migratory capacity, both of which are altered by TGFβ. Cells transfected with *miR-15b* demonstrated increased migration (figure 8D) and attenuated proliferative capacity (not shown).

DISCUSSION

We conducted a comprehensive analysis of miRNA and mRNA expression in whole lung samples from subjects with COPD compared with smokers without COPD and identified 70 differentially expressed miRNAs in COPD tissue compared with tissue from smokers without airflow limitation. *miR-223 and miR-1274a* were the most differentially expressed miRNAs with a near threefold increase in expression in COPD samples. *miR-1274a* has yet to be well described, and recent studies suggest that it harbours significant homology with the transfer RNA Lysine 5 (tRNA ^{Lys5}).[31] tRNAs are primarily responsible for amino acid transfer.[31] Two recent studies demonstrated upregulation of *miR-223* in murine lungs following exposure to aerosolised lipopolysaccharide and downregulation following exposure to cigarette smoke.[7 9]

We compared our list of differentially expressed miRNAs with those previously reported in smokers by Schembri *et al*.[11] The miRNAs that were differentially expressed in our study as well as the previous report included *miR-223, miR-18a, miR-106a, miR-146, miR-99a, miR-150* and *miR-365*. Of these differentially expressed miRNAs, however, *miR-18a* and *miR-365* were the only ones that were increased in expression in both datasets. While the previous study examined airway epithelial cells, we examined whole lung tissue in this study. This may account for the differences in expression patterns. In our study we found increased expression of *miR-146a* in subjects with COPD compared with smokers without obstruction. The previous study by Sato and colleagues reported reduced expression of *miR-146a* in cultured fibroblasts from COPD subjects.[12] Again, this was a cell-specific finding as opposed to our whole lung expression analysis. Lastly, Van Pottelberge *et al* recently identified differences in miRNA expression (including decreased *Let-7c*) in induced sputum from smokers and individuals with COPD.[32] The authors determined that predicted target genes for *Let-7c* were enriched for in sputum from patients with COPD.

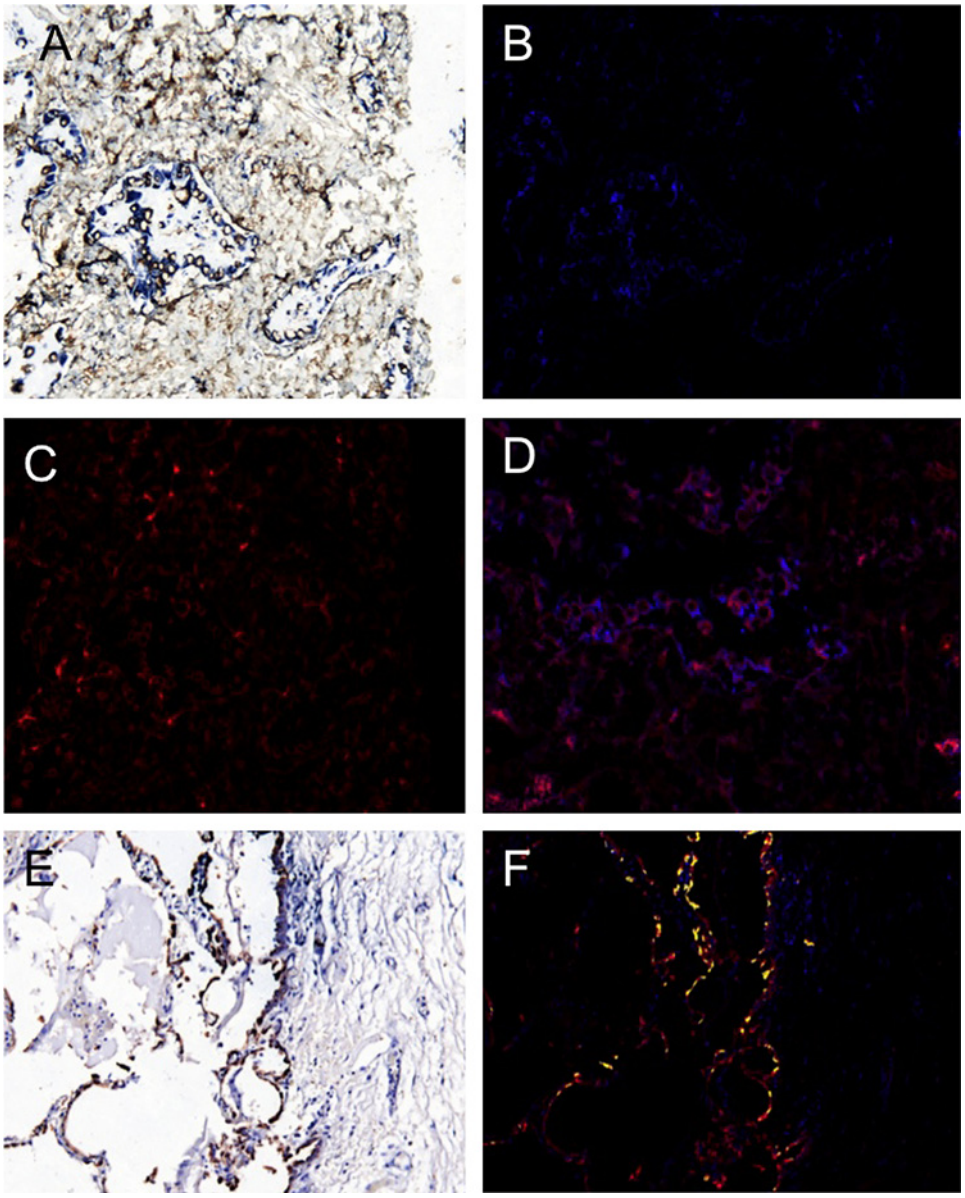

Figure 7 Co-expression of *miR-15b* and mothers against decapentaplegic homologue 7 (Drosophila) (SMAD7) in the lung. This is a representative section of the lung of a subject with chronic obstructive pulmonary disease and associated increased pulmonary fibrosis. All panels are at 200×. (A) Regular colour image after co-expression of *miR-15b* (blue) and SMAD7 (brown). The images were analysed by the Nuance system which converted the *miR-15b* image to fluorescent blue (B) and the SMAD7 image to fluorescent red (C, note the stromal dominance). (D) Mixed image where the absence of fluorescent yellow indicates that the cells expressing *miR-15b* are mutually exclusive from those expressing SMAD7. As a positive control, (E) represents co-expression of *miR-15b* (blue) and AE 1/3 (brown) in the bronchial epithelium. (F) Co-localisation is evident by the intense yellow signal.

Several genes that are part of the TGFβ superfamily were differentially expressed in our data. We identified downregulation of BMP5 and BMP6, TGFβR1 and TGFβR2 and SMAD7. SMAD7 was of particular interest given that it is downregulated in bronchial biopsies of patients with COPD and serves as an inhibitory SMAD in TGFβ signalling.[33] We validated SMAD7 expression in COPD lung tissue by qRT-PCR and by protein in a subset of patients (see figure E4 in online supplement).

miR-15b, *424* and *107*, which were all increased in COPD lung tissue, are members of the *miR15/107* family.[34] Termed the AGCx2 miRNAs because of their common 5′ end (AGCAGC), this group of miRNAs has been implicated in several processes including cell division, stress, angiogenesis and cancer.[34] Lung tissue from patients with GOLD stage 4 COPD had the highest expression of *miR-15b* compared with subjects with other GOLD stages and normal smokers (see figure E1 in online supplement). We demonstrated that overexpression of *miR-15b* in a bronchial epithelial cell line reduced SMAD7, SMURF2 and downstream decorin protein. Conversely, knockdown of *miR-15b* resulted in increased SMAD7, decorin and SMURF2 proteins. Functionally, *miR-15b* manipulation altered early SMAD3 phosphorylation in response to TGFβ treatment.

Wnt (Wingless and Int-1) signalling has been implicated in normal epithelial and mesenchymal function during lung development and dysregulation observed in lung cancer, pulmonary fibrosis and pulmonary hypertension.[35] Dysregulation of several Wnt pathway-related genes in COPD has recently been reported in COPD.[30] Expression of Wnt receptors frizzled homologue (FZD) 5 and FZD 7 were downregulated by 1.76-fold and 1.57-fold, respectively, in our data. With the integration of mRNA and miRNA profiling, we identified several miRNAs that may target the main hubs of this network (see figure E2 in online supplement).

In this study we have presented both mRNA and miRNAs in COPD lung tissue compared with smokers without obstruction. We recognise the limitations of this study, including the lack of phenotypic information of importance such as body composition, frequency of exacerbations, hypoxaemia, perception of dyspnoea or systemic involvement of disease. Our samples were defined by GOLD stages based on spirometric values. There is an inherent limitation in defining patients with COPD by these criteria alone since different phenotypes of disease exist in COPD. We were able to evaluate the available clinical information on these subjects, but factors such as oxygen use, inhaled

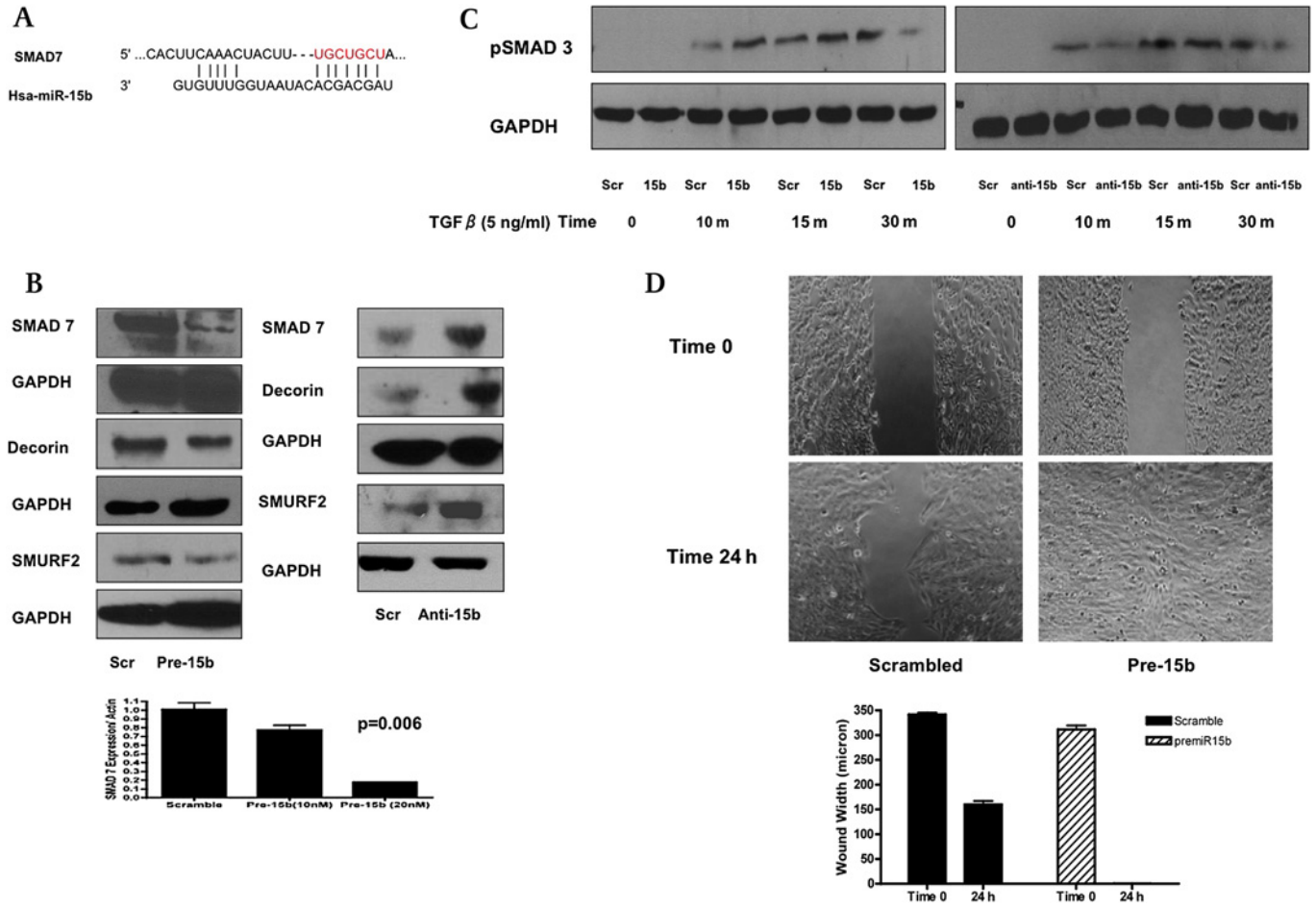

Figure 8 *miR-15B* targeting mothers against decapentaplegic homologue 7 (Drosophila) (SMAD7) in bronchial epithelial cells. (A) Complementarity of 5′ sequence of *miR15-b* and 3′UTR of SMAD7. In Beas2B cells, *miR-15b* overexpression reduced SMAD7 mRNA and protein. *miR-15b* overexpression reduced decorin and SMURF 2 proteins. *miR-15b* knockdown led to increased SMAD7, decorin and SMURF2 proteins. (B) Beas2B cells with *miR-15b* overexpression exhibited increased phosphorylated SMAD3 at 10 and 15 min in response to treatment with transforming growth factor β (TGFβ) (5 ng/ml). Beas2B cells with *miR-15b* knockdown exhibited decreased phosphorylated SMAD3 at 10 and 15 min in response to treatment with TGFβ (5 ng/ml). (C) *miR-15b* overexpression led to increased migratory capacity in Beas2B cells at 24 h. (D) Quantitative reverse transcription polymerase chain reaction is representative of experiments conducted in triplicate. Statistical significance was determined by ANOVA.

steroid use and time since the last cigarette use were not available in the dataset. In addition, we recognise the lack of reproducibility between high throughput studies of the transcriptome and proteome over the past decade.[36–38] These differences may be due to tissue heterogeneity and differences in platforms. However, overall, a few common gene ontology terms are consistently deregulated including cellular organisation and biogenesis, response to stress, organ development, cell adhesion and cellular metabolic process.[36–38]

We propose several miRNAs—including members of the *miR 15/107* family—that deserve further investigation in the regulation of TGFβ signalling in COPD. Expressed miRNAs and mRNAs viewed as networks should generate hypotheses about the key pathologies of inflammation and tissue destruction in this and other diseases of the lung.

Acknowledgements We thank the Lung Tissue Research Consortium (LTRC) for collecting and providing subject specimens.

Funding This work was supported by NIH grant R03 HL095425 (SNS) and by the Flight Attendant Medical Research Institute (FAMRI) (MEE), Pulmonary Systems Biology Initiative of the Battelle Memorial Institute (KW, SZ, RG) as well as support from the University of Luxembourg and the Luxembourg Centre for Systems Biomedicine (DG, KW, JHC, RG).

Competing interests None.

Ethics approval This study was approved by IRB Ohio State University.

Contributors ME, SPN, MC, KW, RG, JC, PD and DG were responsible for preparation of the manuscript; MC, RO and KB conducted in vitro experiments; GN conducted all immunohistochemistry and in situ studies; KW, JC and LY conducted all network and statistical array analysis.

Provenance and peer review Not commissioned; externally peer reviewed.

Data sharing statement All data generated will be uploaded to the appropriate online genomic data banks.

REFERENCES

1. **Fabbri LM,** Hurd SS; GOLD Scientific Committee. Global strategy for the diagnosis, management and prevention of COPD: 2003. *Eur Respir J* 2003;**22**:1—2.
2. **Barnes PJ,** Shapiro SD, Pauwels RA. Chronic obstructive pulmonary disease: molecular and cellular mechanisms. *Eur Respir J* 2003;**22**:672—88.
3. **Ambros V.** The functions of animal microRNAs. *Nature* 2004;**431**:350—5.
4. **Lim LP,** Lau NC, Garrett-Engele P, *et al*. Microarray analysis shows that some microRNAs downregulate large numbers of target mRNAs. *Nature* 2005;**433**:769—73.
5. **Nana-Sinkam SP,** Hunter MG, Nuovo GJ, *et al*. Integrating the MicroRNome into the study of lung disease. *Am J Respir Crit Care Med* 2009;**179**:4—10.
6. **Nana-Sinkam SP,** Karsies T, Riscili B, *et al*. Lung MicroRNA: from development to disease. *Expert Rev Respir Med* 2009;**3**:373—85.
7. **Moschos SA,** Williams AE, Perry MM, *et al*. Expression profiling in vivo demonstrates rapid changes in lung microRNA levels following lipopolysaccharide-induced inflammation but not in the anti-inflammatory action of glucocorticoids. *BMC Genomics* 2007;**8**:240.

8. **Zhai Y,** Zhong Z, Chen CY, *et al*. Coordinated changes in mRNA turnover, translation, and RNA processing bodies in bronchial epithelial cells following inflammatory stimulation. *Mol Cell Biol* 2008;**28**:7414—26.
9. **Izzotti A,** Calin GA, Arrigo P, *et al*. Downregulation of microRNA expression in the lungs of rats exposed to cigarette smoke. *FASEB J* 2009;**23**:806—12.
10. **Izzotti A,** Calin GA, Steele VE, *et al*. Relationships of microRNA expression in mouse lung with age and exposure to cigarette smoke and light. *FASEB J* 2009;**23**:3243—50.
11. **Schembri F,** Sridhar S, Perdomo C, *et al*. MicroRNAs as modulators of smoking-induced gene expression changes in human airway epithelium. *Proc Natl Acad Sci U S A* 2009;**106**:2319—24.
12. **Sato T,** Liu X, Nelson A, *et al*. Reduced MiR-146a increases prostaglandin E2 in chronic obstructive pulmonary disease fibroblasts. *Am J Respir Crit Care Med* 2010;**182**:1020—9.
13. **Bolstad BM,** Irizarry RA, Astrand M, *et al*. A comparison of normalization methods for high density oligonucleotide array data based on variance and bias. *Bioinformatics* 2003;**19**:185—93.
14. **Smyth GK.** Linear models and empirical bayes methods for assessing differential expression in microarray experiments. *Stat Appl Genet Mol Biol* 2004;**3**:Article3.
15. **Storey JD,** Tibshirani R. Statistical significance for genomewide studies. *Proc Natl Acad Sci U S A* 2003;**100**:9440—5.
16. **McClintick JN,** Edenberg HJ. Effects of filtering by Present call on analysis of microarray experiments. *BMC Bioinformatics* 2006;**7**:49.
17. **Kanehisa M,** Goto S. KEGG: kyoto encyclopedia of genes and genomes. *Nucleic Acids Res* 2000;**28**:27—30.
18. **Huang da W,** Sherman BT, Lempicki RA. Systematic and integrative analysis of large gene lists using DAVID bioinformatics resources. *Nat Protoc* 2009;**4**:44—57.
19. **Shannon P,** Markiel A, Ozier O, *et al*. Cytoscape: a software environment for integrated models of biomolecular interaction networks. *Genome Res* 2003;**13**:2498—504.
20. **Nuovo GJ,** Elton TS, Nana-Sinkam P, *et al*. A methodology for the combined in situ analyses of the precursor and mature forms of microRNAs and correlation with their putative targets. *Nat Protoc* 2009;**4**:107—15.
21. **Zandvoort A,** Postma DS, Jonker MR, *et al*. Altered expression of the Smad signalling pathway: implications for COPD pathogenesis. *Eur Respir J* 2006;**28**:533—41.
22. **He JQ,** Foreman MG, Shumansky K, *et al*. Associations of IL6 polymorphisms with lung function decline and COPD. *Thorax* 2009;**64**:698—704.
23. **Kuhn C 3rd,** Homer RJ, Zhu Z, *et al*. Airway hyperresponsiveness and airway obstruction in transgenic mice. Morphologic correlates in mice overexpressing interleukin (IL)-11 and IL-6 in the lung. *Am J Respir Cell Mol Biol* 2000;**22**:289—95.
24. **Tomaki M,** Sugiura H, Koarai A, *et al*. Decreased expression of antioxidant enzymes and increased expression of chemokines in COPD lung. *Pulm Pharmacol Ther* 2007;**20**:596—605.
25. **Churg A,** Wang R, Wang X, *et al*. Effect of an MMP-9/MMP-12 inhibitor on smoke-induced emphysema and airway remodelling in guinea pigs. *Thorax* 2007;**62**:706—13.
26. **Churg A,** Dai J, Tai H, *et al*. Tumor necrosis factor-alpha is central to acute cigarette smoke-induced inflammation and connective tissue breakdown. *Am J Respir Crit Care Med* 2002;**166**:849—54.
27. **He JQ,** Shumansky K, Connett JE, *et al*. Association of genetic variations in the CSF2 and CSF3 genes with lung function in smoking-induced COPD. *Eur Respir J* 2008;**32**:25—34.
28. **Wang IM,** Stepaniants S, Boie Y, *et al*. Gene expression profiling in patients with chronic obstructive pulmonary disease and lung cancer. *Am J Respir Crit Care Med* 2008;**177**:402—11.
29. **Barnes PJ.** The cytokine network in chronic obstructive pulmonary disease. *Am J Respir Cell Mol Biol* 2009;**41**:631—8.
30. **Kneidinger N,** Yildirim AO, Callegari J, *et al*. Activation of the WNT/beta-catenin pathway attenuates experimental emphysema. *Am J Respir Crit Care Med* 2011;**183**:723—33.
31. **Schopman NC,** Heynen S, Haasnoot J, *et al*. A miRNA-tRNA mix-up: tRNA origin of proposed miRNA. *RNA Biol* 2010;**7**:573—6.
32. **Pottelberge GR,** Mestdagh P, Bracke KR, *et al*. MicroRNA expression in induced sputum of smokers and patients with chronic obstructive pulmonary disease. *Am J Respir Crit Care Med* 2011;**183**:898—906.
33. **Springer J,** Scholz FR, Peiser C, *et al*. SMAD-signaling in chronic obstructive pulmonary disease: transcriptional down-regulation of inhibitory SMAD 6 and 7 by cigarette smoke. *Biol Chem* 2004;**385**:649—53.
34. **Finnerty JR,** Wang WX, Hebert SS, *et al*. The miR-15/107 group of microRNA genes: evolutionary biology, cellular functions, and roles in human diseases. *J Mol Biol* 2010;**402**:491—509.
35. **Konigshoff M,** Eickelberg O. WNT signaling in lung disease: a failure or a regeneration signal? *Am J Respir Cell Mol Biol* 2010;**42**:21—31.
36. **Golpon HA,** Coldren CD, Zamora MR, *et al*. Emphysema lung tissue gene expression profiling. *Am J Respir Cell Mol Biol* 2004;**31**:595—600.
37. **Ning W,** Li CJ, Kaminski N, *et al*. Comprehensive gene expression profiles reveal pathways related to the pathogenesis of chronic obstructive pulmonary disease. *Proc Natl Acad Sci U S A* 2004;**101**:14895—900.
38. **Spira A,** Beane J, Pinto-Plata V, *et al*. Gene expression profiling of human lung tissue from smokers with severe emphysema. *Am J Respir Cell Mol Biol* 2004;**31**:601—10.

SUPPLEMENTAL TABLE E1: MICRORNA SEQUENCES USED FOR QRT-PCR.

miRNA	Mature sequence	miRBase Accession	Assay ID
Hsa-miR-1274a	GUCCCUGUUCAGGCGCCA	MIMAT0005927	002883
Hsa-miR-15b	AGGCGGAGACUUGGGCAAUUG	MIMAT0004498	002442
Hsa-miR-424	UGAGAACUGAAUUCCAUGGGUU	MIMAT0000449	000468
Hsa-miR-223	UGUCAGUUUGUCAAAUACCCCA	MIMAT0000280	002295

SUPPLEMENTAL TABLE E2: QRTPCR GENE PROBES

Accession ID	Gene Symbol	Gene	Assay ID
NM_007110.4	TEP1	telomerase-associated protein 1	Hs00200091_m1*
NM_005904.2	SMAD 7	mothers against decapentaplegic homolog 7 (Drosophila),	Hs00998193_m1*
NM_001752.2	CAT	catalase	Hs00156308_m1
NM_000600.3	IL6	interleukin 6 (interferon, beta 2)	Hs00985639_m1*

SUPPLEMENTAL TABLE E3: DIFFERENTIALLY EXPRESSED MICRORNAS (COPD VERSUS NORMAL SMOKERS)

miRNA	logFC	P-value	Q-value
hsa-miR-923	-2.340	5.88E-06	2.91E-05
hsa-miR-937	-1.237	1.89E-06	1.08E-05
hsa-miR-422a	-1.087	1.45E-06	8.74E-06
hsa-miR-576-3p	-1.046	1.57E-06	9.22E-06
hsa-miR-513a-5p	-1.041	3.57E-04	8.54E-04
hsa-miR-25*	-1.006	2.10E-07	1.56E-06
hsa-miR-99b*	-0.853	1.23E-05	5.25E-05
hsa-miR-125b-1*	-0.805	1.38E-05	5.70E-05
hsa-miR-24	-0.804	1.59E-04	4.49E-04
hsa-miR-187*	-0.715	3.14E-04	8.04E-04
hsa-miR-1246	-0.656	3.60E-02	3.35E-02
hsa-miR-1184	-0.620	4.84E-04	1.11E-03
hsa-miR-381	-0.604	1.62E-03	2.74E-03
hsa-miR-107	0.594	7.35E-04	1.45E-03
hsa-miR-142-5p	0.595	2.01E-03	3.24E-03
hsa-miR-99a	0.614	4.16E-03	5.75E-03
hsa-miR-146b-5p	0.632	2.04E-03	3.26E-03
hsa-miR-487b	0.638	6.18E-04	1.30E-03
hsa-miR-1297	0.638	1.16E-02	1.43E-02
hsa-miR-320c	0.645	7.96E-04	1.54E-03
hsa-miR-151-3p	0.648	6.20E-04	1.30E-03
hsa-miR-378	0.648	8.24E-04	1.57E-03
hsa-miR-18b	0.659	1.97E-03	3.20E-03
hsa-miR-642	0.668	8.95E-04	1.69E-03
hsa-miR-193b	0.670	2.55E-04	6.75E-04
hsa-miR-106a	0.675	1.61E-02	1.84E-02
hsa-miR-339-5p	0.682	1.11E-05	4.95E-05
hsa-miR-152	0.690	1.20E-03	2.10E-03
hsa-miR-340	0.702	4.60E-06	2.44E-05
hsa-miR-634	0.712	1.04E-04	3.30E-04
hsa-miR-21	0.714	2.19E-02	2.31E-02
hsa-miR-148b	0.716	2.01E-05	7.84E-05
hsa-miR-518b	0.720	7.92E-06	3.75E-05
hsa-miR-93	0.735	1.55E-04	4.44E-04
hsa-let-7i	0.752	2.36E-05	8.92E-05
hsa-miR-17	0.760	8.06E-03	1.04E-02
hsa-miR-301a	0.764	1.50E-03	2.58E-03
hsa-miR-519d	0.766	7.09E-05	2.32E-04
hsa-miR-150	0.770	9.53E-07	6.06E-06
hsa-miR-28-5p	0.772	1.49E-04	4.35E-04

hsa-miR-625*	0.773	2.20E-06	1.23E-05
hsa-miR-320d	0.789	2.41E-05	8.96E-05
hsa-miR-126*	0.792	3.98E-02	3.61E-02
hsa-miR-374b	0.820	6.04E-04	1.30E-03
hsa-miR-18a	0.826	4.05E-04	9.49E-04
hsa-miR-186	0.829	1.01E-07	8.33E-07
hsa-miR-185	0.856	5.38E-06	2.72E-05
hsa-miR-550	0.874	1.30E-05	5.45E-05
hsa-miR-574-3p	0.876	1.72E-07	1.32E-06
hsa-miR-15b	0.883	9.31E-04	1.73E-03
hsa-miR-214	0.903	7.20E-04	1.43E-03
hsa-miR-142-3p	0.906	1.58E-02	1.83E-02
hsa-miR-424	0.920	2.55E-04	6.75E-04
hsa-miR-342-3p	0.924	6.36E-05	2.11E-04
hsa-miR-365	0.937	2.17E-05	8.35E-05
hsa-miR-146a	0.947	3.23E-05	1.14E-04
hsa-miR-20a	0.955	2.82E-02	2.82E-02
hsa-let-7g	0.956	2.63E-03	4.04E-03
hsa-miR-1260	0.957	4.81E-07	3.24E-06
hsa-let-7d	0.984	6.56E-04	1.37E-03
hsa-miR-451	1.002	5.40E-02	4.59E-02
hsa-miR-10a	1.037	7.47E-04	1.46E-03
hsa-miR-486-5p	1.038	3.26E-04	8.21E-04
hsa-miR-766	1.043	1.05E-05	4.76E-05
hsa-miR-148a	1.107	2.34E-07	1.68E-06
hsa-miR-664	1.146	2.00E-08	2.02E-07
hsa-miR-374a	1.172	1.72E-04	4.74E-04
hsa-miR-144	1.250	2.83E-03	4.26E-03
hsa-miR-1274a	1.450	3.19E-10	4.44E-09
hsa-miR-223	1.550	6.63E-04	1.37E-03

SUPPLEMENTAL TABLE E4: PATHWAYS ENRICHED BY DIFFERENTIALLY EXPRESSED GENES OBTAINED FROM KEGG DATABASE

			DEGs (2667 genes)	PicTar (3583 genes)	PicTar DEGs (635 genes)	TargetScan (6270 genes)	TargetScan DEGs (1100 genes)	miRanda (10380 genes)	miRanda DEGs (1633 genes)
Metabolism	Amino Acid Metabolism	Alanine, aspartate and glutamate metabolism	0.311661	0.967572538	NA	0.47092323	0.61386779	0.38364646	0.17307242
		Arginine and proline metabolism	0.5440286	0.99070845	NA	0.99405651	0.87232242	0.39185541	0.40367693
		Cysteine and methionine metabolism	0.0226454	0.724187326	0.1384449	0.33390341	0.02157677	0.22261954	0.00387908
		Glycine, serine and threonine metabolism	0.1685336	0.967572538	NA	0.99994701	NA	0.99539665	0.58587139
		Histidine metabolism	0.828963	0.998723204	NA	0.99988708	NA	0.99888516	0.94750356
		Lysine biosynthesis	NA	NA	NA	NA	NA	0.95437001	NA
		Lysine degradation	0.9694503	0.279442764	0.8207449	0.51981425	0.95033785	0.63836825	0.98864747
		Phenylalanine metabolism	0.6579092	0.993597504	NA	0.99101413	NA	0.71615537	0.64050278
		Phenylalanine, tyrosine and tryptophan biosynthesis	0.554005	NA	NA	NA	NA	0.23798992	0.39760458
		Tryptophan metabolism	0.5615356	0.999899177	NA	0.99998245	0.93467876	0.99933977	0.54701739
		Tyrosine metabolism	0.6586066	0.99996001	NA	0.99999964	NA	0.99346333	0.81071553
		Valine, leucine and isoleucine biosynthesis	0.5044228	NA	NA	NA	NA	0.98190599	NA
		Valine, leucine and isoleucine degradation	0.3296825	0.999502194	NA	0.99996943	NA	0.89644917	0.62444521
	Carbohydrate Metabolism	Amino sugar and nucleotide sugar metabolism	0.1091182	0.825790271	NA	0.51981425	0.32703908	0.83119358	0.24611359
		Ascorbate and aldarate metabolism	NA	NA	NA	0.99902343	NA	0.99995916	NA
		Butanoate metabolism	NA	0.99604096	NA	0.9991281	NA	0.97706541	NA
		Citrate cycle (TCA cycle)	0.9572843	0.90467567	NA	0.75808056	NA	0.52586002	0.95718673
		Fructose and mannose metabolism	0.3965896	0.724187326	NA	0.47266398	0.66443182	0.73112245	0.64975546
		Galactose metabolism	0.1806852	0.446612567	NA	0.91218998	0.82982813	0.42075739	0.46438499
		Glycolysis / Gluconeogenesis	0.2757824	0.999865207	NA	0.99997689	0.91273671	0.96071094	0.69914125
		Glyoxylate and dicarboxylate metabolism	0.678253	NA	NA	0.92209013	NA	0.99181871	0.78174703
		Inositol phosphate metabolism	0.8363935	0.123125493	0.8789738	0.05924525	0.1407672	0.06587983	0.60580608

		Pentose and glucuronate interconversions	NA	NA	NA	0.99935101	NA	0.97659144	NA
		Pentose phosphate pathway	0.5239334	0.996790886	NA	0.99665347	0.49595759	0.49267581	0.70962248
		Propanoate metabolism	0.8761501	0.994054055	NA	0.99969581	NA	0.99709965	NA
		Pyruvate metabolism	0.5615356	0.999899177	NA	0.99999832	NA	0.9720779	0.9094099
		Starch and sucrose metabolism	0.8913046	0.995549632	NA	0.9955899	0.77340283	0.89753227	0.78461105
	Energy Metabolism	Methane metabolism	0.2212647	NA	NA	0.65090358	NA	0.72406742	0.45570965
		Nitrogen metabolism	0.6882821	0.878537841	NA	0.52347571	0.79114736	0.186068	0.38453636
		Oxidative phosphorylation	0.9984703	0.999999999	NA	0.99999998	0.99987029	0.99999342	0.99999841
		Sulfur metabolism	0.8561989	NA	NA	NA	NA	0.95723606	0.7039721
	Glycan Biosynthesis and Metabolism	Chondroitin sulfate biosynthesis	0.9715394	0.858240226	NA	0.29611107	NA	0.38909151	0.89290476
		Glycosaminoglycan degradation	0.9665294	0.948157826	NA	0.98759598	NA	0.98261375	NA
		Glycosylphosphatidylinositol(GPI)-anchor biosynthesis	0.905463	0.996790886	NA	0.95514373	NA	0.943536	0.70962248
		Heparan sulfate biosynthesis	NA	0.272583491	NA	0.0093115	NA	0.42075739	NA
		Keratan sulfate biosynthesis	0.3482235	0.318017913	NA	0.31285447	0.61419341	0.01345136	0.14582827
		N-Glycan biosynthesis	0.5398948	0.473567596	0.8342778	0.89028684	NA	0.52892882	0.45951626
		O-Glycan biosynthesis	0.673976	0.418463643	0.6897429	0.27953146	0.59576837	0.05263959	0.32672083
		O-Mannosyl glycan biosynthesis	NA	NA	NA	NA	NA	0.90123868	NA
		Other glycan degradation	0.0770167	NA	NA	NA	NA	0.98100943	0.80284051
	Lipid Metabolism	alpha-Linolenic acid metabolism	0.9455708	0.983930923	NA	0.99345461	NA	0.9934561	NA
		Arachidonic acid metabolism	0.6100163	0.999701117	NA	0.99999686	0.97820527	0.99915603	0.97659095
		Biosynthesis of unsaturated fatty acids	0.9715394	0.479570702	NA	0.64207289	0.77639651	0.71615537	0.89290476
		Ether lipid metabolism	0.614037	0.87192699	NA	0.52086642	0.90801792	0.7850852	0.86448595
		Fatty acid biosynthesis	NA	NA	NA	0.9131115	NA	0.92220498	NA
		Fatty acid elongation in mitochondria	NA	NA	NA	NA	NA	0.8996091	NA
		Fatty acid metabolism	0.5615356	0.856599141	NA	0.99766071	NA	0.99802643	0.9094099
		Glycerolipid metabolism	0.92	0.92230455	NA	0.68298814	0.9536283	0.86632623	0.98975097
		Glycerophospholipid metabolism	0.9525307	0.539144792	NA	0.16461694	0.83396318	0.31844826	0.90490466
		Linoleic acid metabolism	0.6181022	NA	NA	0.99998916	NA	0.99952295	NA
		Primary bile acid biosynthesis	NA	NA	NA	0.94184237	NA	0.52297924	NA

		Sphingolipid metabolism	0.7110419	0.713702036	NA	0.19931078	0.73671383	0.92501936	0.90171955
		Steroid biosynthesis	NA	NA	NA	0.99064624	NA	0.96238054	NA
		Steroid hormone biosynthesis	0.9279369	0.999974822	NA	0.99991178	0.95670135	0.99283973	0.9907474
		Synthesis and degradation of ketone bodies	NA	NA	NA	NA	NA	0.81463094	NA
	Metabolism of Cofactors and Vitamins	Folate biosynthesis	0.8309438	NA	NA	NA	NA	0.80398918	NA
		Nicotinate and nicotinamide metabolism	NA	0.970857003	NA	0.86453326	NA	0.71842558	NA
		One carbon pool by folate	0.0770167	NA	NA	0.83649711	0.28347395	0.94065479	0.19514931
		Pantothenate and CoA biosynthesis	0.911516	0.967974979	NA	0.79343415	NA	0.41370945	NA
		Porphyrin and chlorophyll metabolism	0.3681382	NA	NA	0.99997524	0.89453214	0.99947459	0.62926795
		Retinol metabolism	0.5665434	0.999556534	0.8789738	0.99831155	0.9749951	0.99925923	0.90437227
		Riboflavin metabolism	0.7130814	NA	NA	0.94184237	0.66334649	0.94065479	0.4653448
		Thiamine metabolism	0.3398706	NA	NA	0.26053334	0.41952396	0.8996091	0.17604164
		Vitamin B6 metabolism	NA	NA	NA	NA	NA	0.92220498	NA
	Metabolism of Other Amino Acids	beta-Alanine metabolism	0.4199366	0.993597504	NA	0.99846762	NA	0.98921265	0.89290476
		Cyanoamino acid metabolism	NA	NA	NA	NA	NA	0.95882864	NA
		D-Glutamine and D-glutamate metabolism	0.4758037	0.188032749	NA	0.40915597	NA	0.37094314	0.33331058
		Glutathione metabolism	0.3245158	0.995585114	NA	0.99988324	0.96709221	0.75192869	0.87348682
		Selenoamino acid metabolism	0.0805838	0.446612567	0.0747107	0.91218998	0.24178987	0.72083153	0.2375278
		Taurine and hypotaurine metabolism	0.80126	0.899025627	NA	0.70338694	NA	0.24035684	NA
	Metabolism of Terpenoids and Polyketides	Limonene and pinene degradation	NA	0.959702511	NA	0.99667466	NA	0.98557335	NA
		Terpenoid backbone biosynthesis	NA	0.967974979	NA	0.92209013	NA	0.90831268	NA
	Nucleotide Metabolism	Purine metabolism	0.9942811	0.999728592	NA	0.99238311	0.99233476	0.73250191	0.99940274
		Pyrimidine metabolism	0.9992145	0.999893832	NA	0.99947546	0.98844901	0.96243364	0.99993998
	Xenobiotics Biodegradation and Metabolism	Metabolism of xenobiotics by cytochrome P450	0.2757824	NA	NA	1	NA	0.99999993	0.98350292
Genetic Information Processing	Folding, Sorting and Degradation	Proteasome	0.9954466	0.992575817	NA	0.99993632	0.95957131	0.91936905	0.99164714
		RNA degradation	0.3402992	0.757960461	NA	0.66506391	0.89714571	0.98521611	0.99700056
		SNARE interactions in vesicular transport	0.9978842	0.00193665	NA	0.02497689	0.92509131	0.09106122	NA

		Ubiquitin mediated proteolysis	0.2997347	0.002805588	0.2676058	2.483E-05	0.28790931	2.2676E-06	0.10664352
	Replication and Repair	Base excision repair	0.787815	0.996773151	NA	0.97381745	NA	0.99376278	0.9715315
		DNA replication	0.4531702	NA	NA	0.99954654	0.91410148	0.97531258	0.87485135
		Homologous recombination	NA	NA	NA	0.99998916	NA	0.95833912	NA
		Mismatch repair	0.8777988	NA	NA	0.69395916	0.79114736	0.78321633	NA
		Non-homologous end-joining	NA	NA	NA	0.99499818	NA	0.99468494	NA
		Nucleotide excision repair	0.9112891	0.962950953	NA	0.91458303	0.79531769	0.96919545	0.93487758
	Transcription	Basal transcription factors	0.9965532	0.428206219	NA	0.66079094	NA	0.67398541	0.9715315
		RNA polymerase	0.98925	NA	NA	0.99878576	NA	0.91153755	NA
		Spliceosome	0.172141	0.88373349	0.5296777	0.54351042	0.59283554	0.30974005	0.22961395
	Translation	Aminoacyl-tRNA biosynthesis	0.0740458	0.999919981	NA	0.99956327	NA	0.99650021	0.91653449
		Ribosome	0.0285019	0.999999998	NA	1	NA	1	0.99252332
Environmental Information Processing	Membrane Transport	ABC transporters	0.8062986	0.279442764	NA	0.75796166	0.95033785	0.96919545	0.81071553
		Protein export	0.3398706	NA	NA	0.80672925	0.41952396	0.4482186	0.17604164
	Signal Transduction	Calcium signaling pathway	0.7168691	0.016803733	0.0356407	0.00383646	0.17899261	0.02337471	0.53465037
		ErbB signaling pathway	0.2168246	0.000119414	0.2372793	1.046E-06	0.21035646	0.0005804	0.32687001
		Hedgehog signaling pathway	0.6100163	0.155800837	0.8881285	0.00332365	0.97820527	0.01100783	0.45694259
		Jak-STAT signaling pathway	0.2857191	0.041090108	0.3791778	0.06794411	0.1382218	0.00135203	0.23380411
		MAPK signaling pathway	0.0892441	8.01592E-13	0.0001752	1.869E-13	0.02643733	2.2419E-06	0.02222242
		mTOR signaling pathway	0.5210647	0.161434765	0.5961856	0.00026373	0.25422383	0.05964617	0.75208755
		Notch signaling pathway	0.0807335	0.043288559	0.2660992	0.0015783	0.08501119	0.00033012	0.16179571
		Phosphatidylinositol signaling system	0.7941028	0.010211541	0.5412452	0.00450758	0.11041484	0.0195404	0.42168818
		TGF-beta signaling pathway	0.0148621	2.0855E-07	9.704E-05	9.7057E-09	0.00141885	5.2799E-06	0.00335242
		VEGF signaling pathway	0.1398929	0.072614661	0.1570074	0.01129742	0.1169664	0.22987649	0.43686868
		Wnt signaling pathway	0.3150003	1.43633E-11	0.1216808	1.4779E-14	0.00434116	7.7884E-10	0.03101041
	Signaling Molecules and Interaction	Cell adhesion molecules (CAMs)	0.0304223	0.450487834	0.2383063	0.15768726	0.7741984	0.12388085	0.19945078
		Cytokine-cytokine receptor interaction	0.0065022	0.739618116	0.79173	0.86200225	0.36043497	0.00864035	0.04210011
		ECM-receptor interaction	0.0375566	0.000338015	0.0402435	0.00053073	0.09808704	0.00140553	0.00566799
		Neuroactive ligand-receptor interaction	0.9999997	0.973466563	0.997506	0.95112038	0.99954736	0.96538516	0.99999949
Cellular Processes	Cell Communication	Adherens junction	0.0075503	0.000350679	0.0723646	1.2472E-08	0.00401871	7.172E-05	0.01402062
		Focal adhesion	9.955E-07	8.7584E-10	4.463E-07	4.1196E-12	1.9084E-07	2.0365E-06	7.2735E-07
		Gap junction	0.3448553	0.002275947	0.2516694	0.00025787	0.70487626	0.03104375	0.49194213
		Tight junction	0.4380605	0.010125141	0.0691094	0.00120049	0.78735902	0.02162008	0.41644951

	Cell Growth and Death	Apoptosis	0.0882777	0.726717786	0.8514449	0.00956359	0.68559935	0.15275183	0.746748
		Cell cycle	0.3098195	0.015562841	0.1992744	0.02121993	0.3048835	0.03018412	0.31644053
		Oocyte meiosis	0.9121378	0.003122052	0.2421787	1.9531E-05	0.18423977	0.00067228	0.62602013
		p53 signaling pathway	0.435183	0.050004703	0.2603295	0.00670619	0.15657617	0.0135151	0.20432311
	Cell Motility	Regulation of actin cytoskeleton	0.0057287	3.55766E-06	1.805E-05	1.8053E-12	7.9426E-06	7.5121E-08	0.0002864
	Transport and Catabolism	Endocytosis	0.0711887	3.00916E-06	0.0227307	5.0149E-11	0.00418808	6.2378E-06	0.01661282
		Lysosome	0.2077767	0.624321399	0.8310009	0.14309702	0.36135972	0.91745848	0.23385201
		Regulation of autophagy	0.9965532	0.87192699	NA	0.93872653	0.90801792	0.96479057	NA
Organismal Systems	Circulatory System	Cardiac muscle contraction	0.9127193	0.65247628	0.5773296	0.96933145	0.96851291	0.89317852	0.98450256
		Vascular smooth muscle contraction	0.0221258	0.06309534	0.0631106	0.00142677	0.06227142	0.08094742	0.06930892
	Development	Axon guidance	0.3658191	1.82268E-14	0.000353	1.6545E-11	0.02105085	1.6506E-12	0.06803939
		Dorso-ventral axis formation	0.5239334	0.406452011	0.2467852	0.00567038	0.22394222	0.10850217	0.43820916
	Endocrine System	Adipocytokine signaling pathway	0.4148339	0.001031577	0.4741344	6.8834E-05	0.0704503	0.00033494	0.31595315
		GnRH signaling pathway	0.7199286	0.000669023	0.5183442	9.6316E-05	0.78131945	0.03504321	0.47417146
		Insulin signaling pathway	0.3590868	0.000274884	0.0717166	1.3172E-05	0.05823813	0.00010169	0.4277422
		Melanogenesis	0.891154	4.70945E-08	0.5264305	5.6048E-07	0.47726998	0.00038001	0.62451647
		PPAR signaling pathway	0.7197313	0.781583062	0.4937822	0.8197549	0.47801977	0.46234552	0.50251883
		Progesterone-mediated oocyte maturation	0.9552766	0.147258613	0.6439742	0.0075539	0.50098285	0.05588655	0.92770052
		Renin-angiotensin system	0.744691	NA	NA	0.8717646	0.68552883	0.7881019	0.82189913
	Environmental Adaptation	Circadian rhythm	0.5983604	0.000196309	0.085714	0.00893816	0.58699641	0.02178893	0.36085283
	Excretory System	Aldosterone-regulated sodium reabsorption	0.2601385	0.322686333	0.2047037	0.00227351	0.04921977	0.0795628	0.36076854
	Immune System	Antigen processing and presentation	0.1029432	0.99978364	0.9614344	0.99997803	0.64457579	0.99821961	0.17186944
		B cell receptor signaling pathway	0.1398929	0.180742568	0.5504305	0.03542911	0.05554549	0.16501933	0.59383183
		Chemokine signaling pathway	0.0096608	0.014004786	0.1757481	0.00033376	0.01034982	0.00539078	0.02020896
		Complement and coagulation cascades	0.7197313	0.999375463	NA	0.99969994	0.9910901	0.94547402	0.96859155
		Cytosolic DNA-sensing pathway	0.7322961	0.998182262	NA	0.99079218	NA	0.97266548	0.91094728
		Fc epsilon RI signaling pathway	0.2665985	0.102469157	0.5773296	0.00078471	0.06807797	0.10104242	0.48203998
		Fc gamma R-mediated phagocytosis	0.2426728	0.006730518	0.2960199	1.9333E-06	0.02072694	0.00118922	0.30594341

		Hematopoietic cell lineage	0.295193	0.977429453	0.9657507	0.88827216	0.98027765	0.05588655	0.44965596
		Intestinal immune network for IgA production	0.3025375	0.954142698	NA	0.93458111	0.96475465	0.37117205	0.33233329
		Leukocyte transendothelial migration	0.0129862	0.110471074	0.0140559	0.00569311	0.02165608	0.12876412	0.0168581
		Natural killer cell mediated cytotoxicity	0.2497848	0.975298846	0.8894145	0.97023719	0.78085159	0.89148856	0.90614911
		NOD-like receptor signaling pathway	0.0011909	0.276759293	0.086417	0.51870423	0.10989388	0.20905455	0.0052846
		RIG-I-like receptor signaling pathway	0.4957657	0.814297673	0.7610337	0.32372772	0.85501597	0.56521771	0.69281814
		T cell receptor signaling pathway	0.7562246	0.008016051	0.5960581	5.6559E-07	0.27760697	0.00027482	0.83062314
		Toll-like receptor signaling pathway	0.2399534	0.508093121	0.5424058	0.35235921	0.66026121	0.87887546	0.77081459
	Nervous System	Long-term depression	0.3281182	0.097259743	0.7468893	0.00880999	0.47801977	0.00519551	0.21647774
		Long-term potentiation	0.8152479	2.47945E-05	0.2603295	1.1061E-07	0.46505319	2.8417E-05	0.65139088
		Neurotrophin signaling pathway	0.1028205	2.55899E-07	0.0073249	5.1881E-14	0.01510896	1.7766E-06	0.13793821
	Sensory System	Olfactory transduction	NA	1	NA	1	NA	1	NA
		Taste transduction	NA	0.989102986	NA	0.9971749	NA	0.99832142	NA
Human Diseases	Cancers	Acute myeloid leukemia	0.3614365	0.008836168	0.1791375	1.9246E-06	0.08357276	0.07879201	0.49183333
		Basal cell carcinoma	0.928799	0.00450669	0.8836407	4.4334E-05	0.492517	0.14253932	0.91094728
		Bladder cancer	0.0395284	0.071761912	0.2147159	0.01890844	0.29665409	0.18250788	0.21361571
		Chronic myeloid leukemia	0.2194776	0.000521101	0.1570074	1.2941E-08	0.05554549	0.0041198	0.29455148
		Colorectal cancer	0.0668489	2.2991E-06	0.0402435	5.5246E-09	0.002977	0.00290768	0.18180411
		Endometrial cancer	0.8083143	0.025985764	0.8690741	8.9546E-05	0.67383017	0.44124536	0.99499327
		Glioma	0.6099619	0.005219077	0.433862	2.3849E-07	0.23097475	0.04501964	0.73966332
		Melanoma	0.4957657	0.042876434	0.2860197	0.00014299	0.18284592	0.03863662	0.53380234
		Non-small cell lung cancer	0.8363935	0.03714777	0.8789738	2.5997E-05	0.69872371	0.17088388	0.97215683
		Pancreatic cancer	0.2697612	0.000236643	0.0555982	1.1153E-05	0.04461884	0.00923889	0.39126895
		Pathways in cancer	9.995E-07	7.72089E-15	1.43E-08	1.0844E-24	2.0888E-08	1.0609E-12	7.4017E-08
		Prostate cancer	0.2453521	0.001056823	0.4430297	9.1293E-09	0.06521889	0.00070344	0.35332166
		Renal cell carcinoma	0.012183	1.52755E-06	0.0012304	2.7703E-08	0.00176105	4.0375E-05	0.00602412
		Small cell lung cancer	0.0046861	5.3057E-05	0.0003037	5.5246E-09	0.00099633	0.00140553	0.01317236
		Thyroid cancer	0.828963	0.056069596	NA	0.00039522	0.86136243	0.03159751	0.94750356
	Cardiovascular Diseases	Arrhythmogenic right ventricular cardiomyopathy (ARVC)	0.4631528	3.78622E-05	0.3295531	0.00192625	0.56530264	0.09511073	0.1926222
		Dilated cardiomyopathy	0.3960538	0.0040041	0.2736494	0.01626201	0.8638423	0.00939212	0.1717675

		Hypertrophic cardiomyopathy (HCM)	0.3870356	0.000991134	0.1045814	0.03222358	0.81935933	0.04276553	0.19200117
		Viral myocarditis	0.0011177	0.610292151	0.513064	0.85900863	0.50362778	0.65664305	0.14150089
	Immune System Diseases	Allograft rejection	0.1571998	0.986596064	NA	0.89755203	NA	0.3521654	0.87485135
		Asthma	0.1294083	0.998723204	NA	0.95632634	0.86136243	0.51555917	0.30405525
		Autoimmune thyroid disease	0.4977123	0.999202443	NA	0.99878035	NA	0.98733125	0.9639561
		Graft-versus-host disease	0.1157606	0.992237035	NA	0.99688976	NA	0.43368342	0.52640705
		Primary immunodeficiency	0.614037	0.999680068	NA	0.93872653	0.90801792	0.98431873	0.9715315
		Systemic lupus erythematosus	0.4043481	0.999997643	NA	0.99999029	0.96300116	0.98542253	0.98925282
	Infectious Diseases	Epithelial cell signaling in Helicobacter pylori infection	0.8152479	0.027273025	0.2603295	0.01303399	0.66218451	0.04373349	0.65139088
		Pathogenic Escherichia coli infection	0.3402992	0.380769215	0.1715387	0.16515094	0.3191219	0.31132468	0.6544757
		Vibrio cholerae infection	0.6100163	0.737214551	0.8881285	0.14130825	0.97820527	0.02215317	0.45694259
	Metabolic Diseases	Maturity onset diabetes of the young	0.9825058	0.602602989	NA	0.18023522	NA	0.78278205	NA
		Type I diabetes mellitus	0.163556	0.982774633	NA	0.96971918	NA	0.11109846	0.78461105
		Type II diabetes mellitus	0.1521473	0.083523109	0.2660992	0.00908693	0.08501119	0.17136383	0.16179571
	Neurodegenerative Diseases	Alzheimer's disease	0.3048037	0.992706367	0.8763121	0.98011127	0.63660083	0.83651915	0.71662427
		Amyotrophic lateral sclerosis (ALS)	0.5440286	0.031199375	0.3293427	0.01289052	0.46331657	0.02510449	0.40367693
		Huntington's disease	0.6033852	0.977428582	0.3806216	0.99500188	0.8466651	0.78930485	0.89768033
		Parkinson's disease	0.9889915	0.999999993	0.9935487	0.99999999	0.99847202	0.99905861	0.99997055
		Prion diseases	0.787815	0.87192699	NA	0.52086642	NA	0.05419744	0.86448595

P>0.05	
0.0005<=P<=0.05	
P<0.0005	

* Pathway enrichment analysis was performed in DAVID

* Multiple testing correction was not applied

A

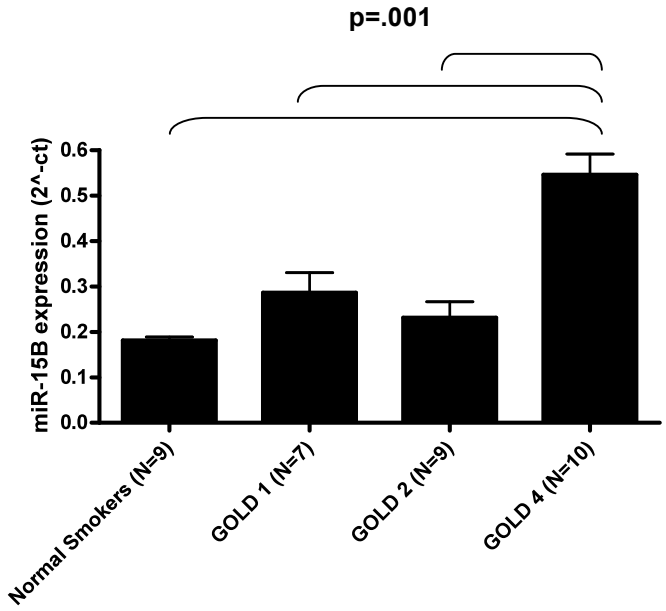

B.

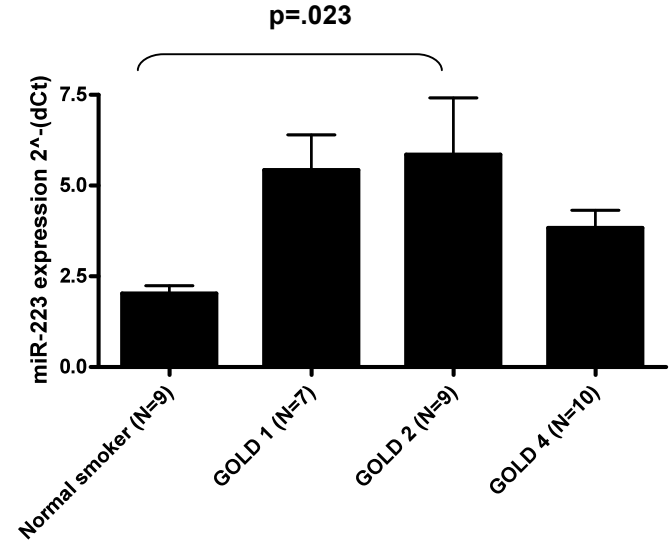

Supplemental Figure E1

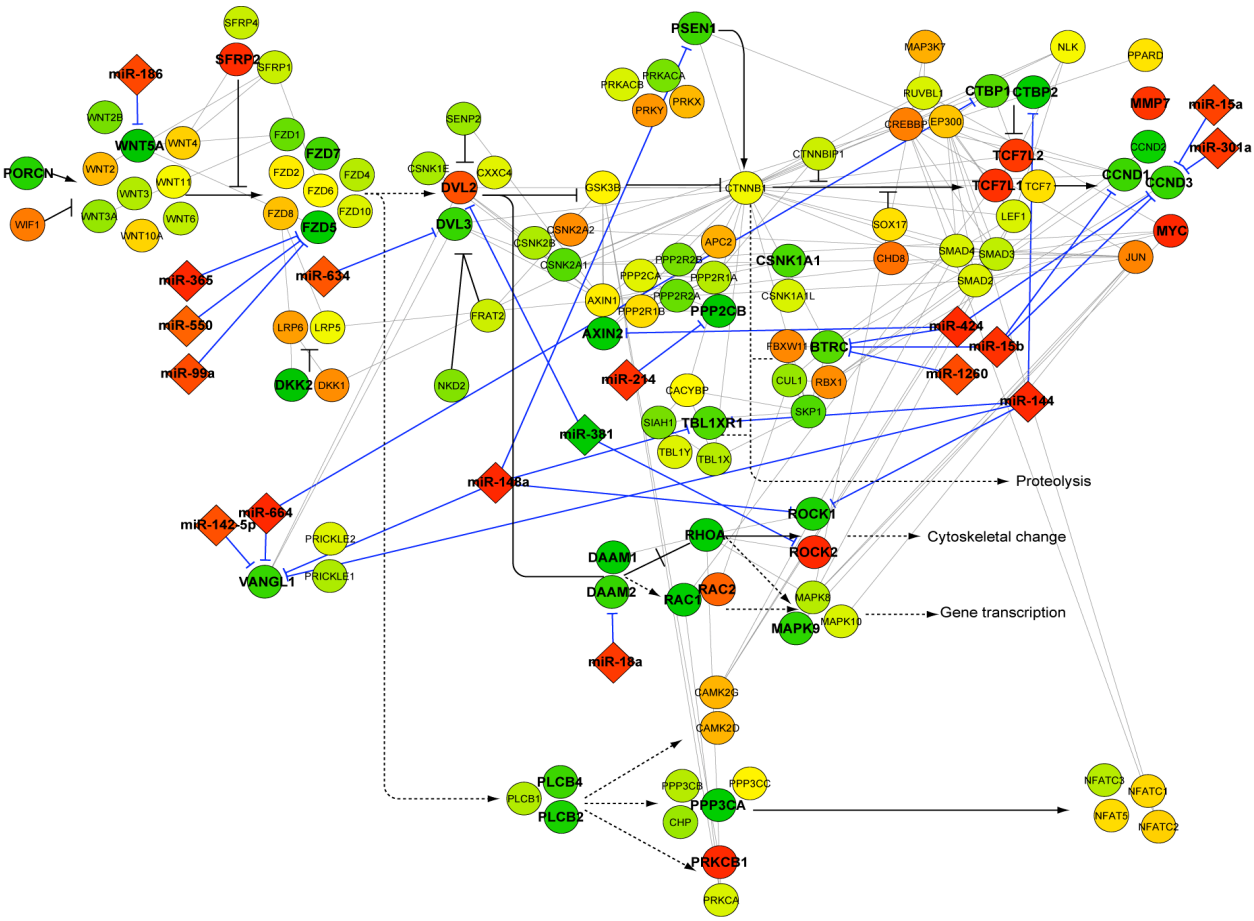

Supplemental Figure E2

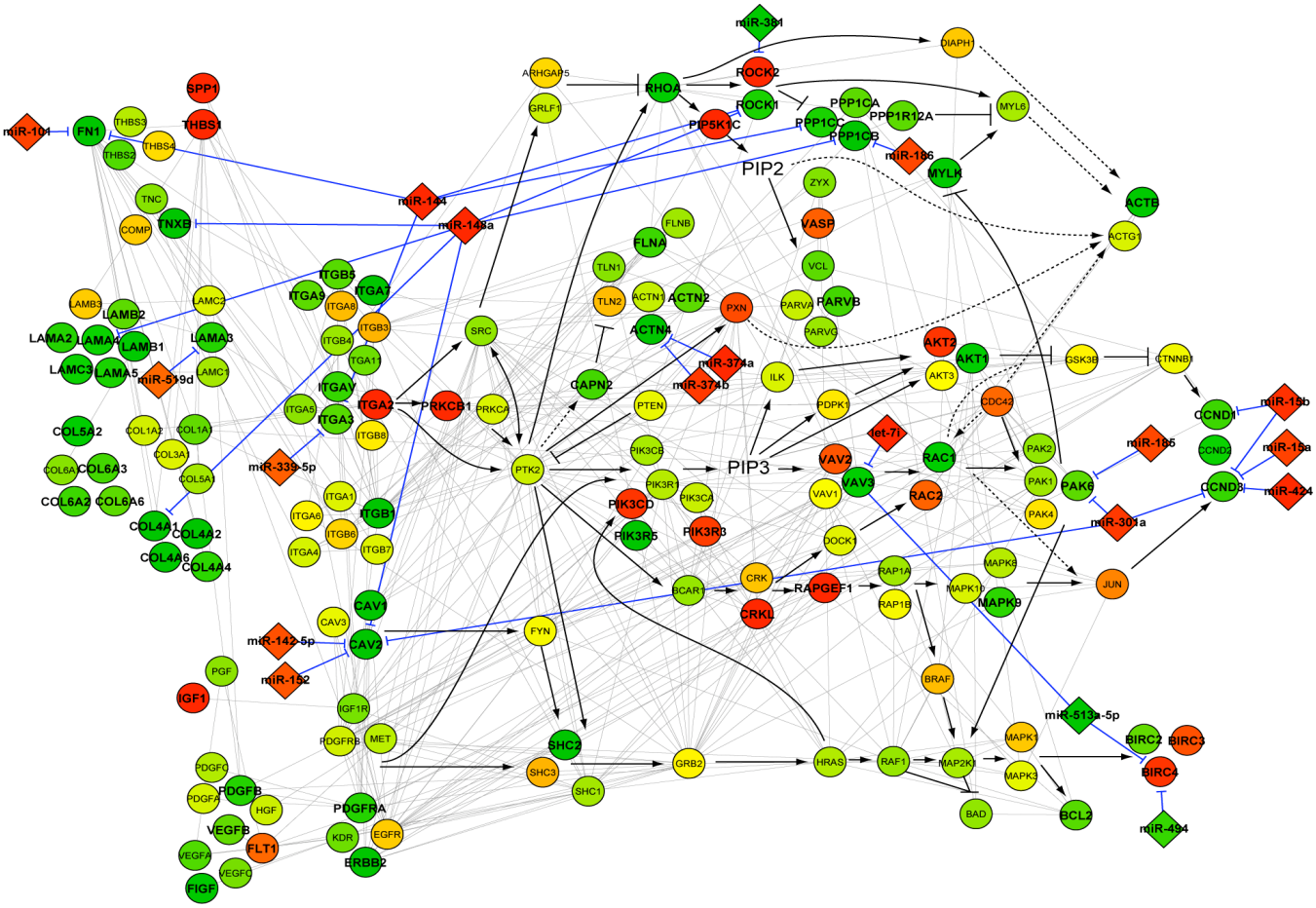

Supplemental Figure E3

GOLD	Average FEV1/FVC	Standard Deviation
4	0.34	0.12
2	0.58	0.074
1	0.64	0.045
Normal Smokers	0.77	0.05

Supplemental Table E5

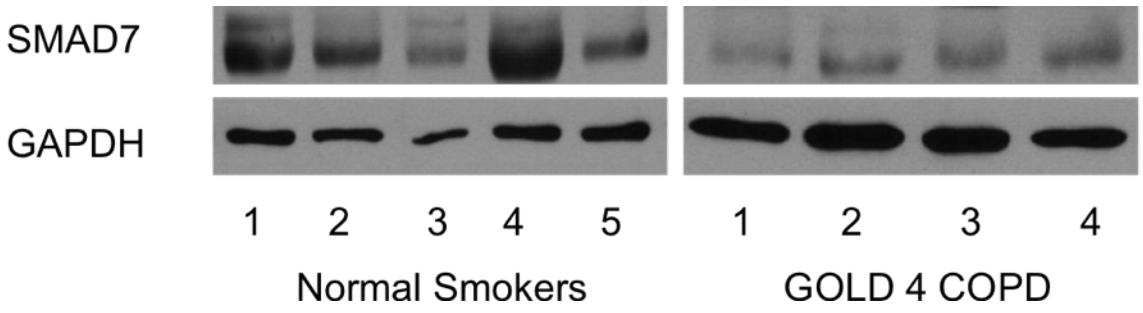

Supplemental Figure E4

GOLD STAGE	GOLD STAGE	Difference	Adjusted p-value
Normal Smokers	**1**	-6.4921	0.4094
Normal Smokers	**2**	-5.8889	0.4363
Normal Smokers	**4**	12.3222	0.0133
1	**2**	0.6032	0.9989
1	**4**	18.8143	0.0003
2	**4**	18.2111	0.0002

Supplemental Table E6

GOLD STAGE	GOLD STAGE	Difference	Adjusted p-value
Normal Smokers	**1**	-16.1905	0.6092
Normal Smokers	**2**	-18.3333	0.4781
Normal Smokers	**4**	-30.7333	0.0686
1	**2**	-2.1429	0.9985
1	**4**	-14.5429	0.6708
2	**4**	-12.4000	0.7471

Supplemental Table E7

GOLD STAGE	GOLD STAGE	Difference	Adjusted p-value
Normal Smokers	**1**	15.2222	0.0193
Normal Smokers	**2**	33.6667	<.0001
Normal Smokers	**4**	83.0222	<.0001
1	**2**	18.4444	0.0035
1	**4**	67.8000	<.0001
2	**4**	49.3556	<.0001

Supplemental Table E8

Supplemental Material

METHODS

miRNA Microarray

MiRNAs were profiled in both COPD (N=19) and Normal Smokers (N=8) using Exiqon miRNA microarrays as per the manufacturer's instructions (Exiqon, Woburn, MA). In brief, 15µL of total RNA was labeled using the miRCURY LNA microRNA Power Labeling Kit (Exiqon, Woburn, MA). The RNA was dephosphorylated with calf intestinal alkaline phosphatase and denatured by heating to 95ºC. Hy3 or Hy5 dyes were ligated to the dephosphorylated single-stranded RNA. The labeled miRNA probes were hybridized to the miRCURY LNA arrays v.11.0 for 16 hours at 56º C. After hybridization, the arrays were washed and scanned at 5µm resolution using a ScanArray Express (Perkin Elmer, Waltham, MA).

Messenger RNA Microarray

Samples were prepared for mRNA microarray analysis using Agilent Quick Amp Labeling technologies (Santa Clara, CA), which uses T7 polymerase to amplify targets and cyanine 3- or cyanine 5- to fluorescently label RNA targets. Approximately 500 ng of RNA was used in the labeling and amplification reactions. Following the labeling and amplification of the samples, Qiagen's RNeasy mini kit (Valencia, CA) was used to purify the labeled cRNA. The purified cRNA was then quantified using the NanoDrop

ND- 1000 UV-Vis Spectrophotometer (Wilmington, DE), and the yield and specific activity of labeled targets were calculated. The labeled cDNA targets were fragmented, mixed with hybridization buffer, and incubated at 65°C overnight. The hybridized slides were then washed and scanned with ScanArray Express (Perkin Elmer, Waltham, MA).

mRNA and miRNA microarray data processing

For mRNA data, raw intensities from all samples were merged, normalized using quantile method, and transformed into log2-scale . Present probes with mean intensity over all samples larger than the global mean intensity were chosen and used for further statistical analysis. As for miRNA data, the intensity for each miRNA was computed by taking median value of four replicates since each miRNA on the microarray has four identical replicated probes. MiRNA hybridization intensities were processed as described above for mRNA.

LIMMA and QVALUE , R packages were used to perform statistical testing of differential mRNA and miRNA expression between control smoker and COPD samples and compute positive false discovery rate (pFDR), respectively. We used present probes for statistical testing to increase the ratio of true positives to false positives and defined differentially expressed mRNAs and miRNAs as having pFDR<0.05 with at least ±1.5 fold-change between the groups. For multiple probes mapped to the same Entrez ID or miRNA symbol, the probe with the smallest pFDR value was chosen to represent the differentially expressed mRNA and miRNA.

In Situ Hybridization and Co-localization

In brief, the in situ hybridization was done following a protease digestion that utilizes a probe cocktail containing 1 pmol/microL of the 5' digoxigenin labeled LNA probe (Exiqon). Following an overnight hybridization and development in NBT/BCIP, SMAD7 was assessed using a 30 minute antigen retrieval and a dilution of 1:200 and AE 1/3 (Dako) 1:100 with a 1 hour and 30 minute incubation. After development via peroxidase/DAB, the slide was analyzed with the Nuance system (Cambridge Research Institute).

Transfection Studies and Western

Beas2Bs (bronchial epithelial cell line) were cultured in RPMI (Fisher Manassas, Va.) with 10% fetal bovine serum and Penicillin/Streptomycin and maintained at 37ºC humidified 5% CO_2 chamber. Transfection with scramble, pre-miR15b or anti-miR15b was performed using Lipofectamine (Invitrogen Carlsbad, Ca.) following manufacturer's protocol at the specified concentrations. The media was replaced within 24 hours to reduce the toxicity of the transfection complex. Cells were harvested at 24 hours and assessed by QRT-PCR for adequate *miR-15b* induction. Cells were harvested after 72 hours in RIPA with the addition of phosphatase and protease inhibitors. Protein expression of SMAD7 (Santa Cruz, Ca.), SMURF 2 (Sigma, St. Louis, MO.) and Decorin (Cell Signaling, Danvers, MA.) were then determined by SDS-PAGE.

Migration Assay

Migration rate was assayed using the IBIDI culture insert (München, Germany). The migration insert was set into a 24 well plate. 20K cells were transfected with either scrambled miR or pre-miR15b and suspended in 80ul of media and plated into each well. After 16 hours, the insert was removed and the cells were washed 6 times to remove any non-adherent cells and replaced with full media. Images were taken on an Olympus IX81 immediately (Time 0) and again at 8 and 24 hours. Seven random widths were measured across the wound at Time 0. The number of pixels was converted to microns and the line was then superimposed onto the subsequent time points. The mean and standard deviation of the 7 lines was then calculated using ImageJ software to determine distance of wound closure. Experiments were performed in triplicate

Results

Study Subjects

Study subjects were grouped according to GOLD classification based on the reported post-bronchodilator FEV1 (forced expiratory volume in one second) percent predicted. All of the COPD subjects by definition had an FEV1/FVC ratio less than the age-predicted reference normal values. The smokers without airflow limitation had a normal FEV1/FVC ratio.